ROLE OF CURRENT DENSITY IN IMPRESS CURRENT CATHODIC PROTECTION OF STAINLESS STEEL IN 3.5% NaCl SOLUTION

JUSTIN GERARD A/L K.GERARD

FACULTY OF ENGINEERING
UNIVERSITY OF MALAYA
KUALA LUMPUR

2015

ROLE OF CURRENT DENSITY IN IMPRESS CURRENT CATHODIC PROTECTION OF STAINLESS STEEL IN 3.5% NaCl SOLUTION

JUSTIN GERARD A/L K.GERARD

RESEARCH REPORT SUBMITTED IN PARTIAL FULFILLMENT OF THE REQUIREMENT FOR THE DEGREE OF MASTER OF ENGINEERING

FACULTY OF ENGINEERING
UNIVERSITY OF MALAYA
KUALA LUMPUR

2015

UNIVERSITY OF MALAYA

ORIGINAL LITERARY WORK DECLARATION

Name of Candidate: **Justin Gerard A/L K.Gerard** (I.C/Passport No:

Registration/Matric No: **KMB 130010**

Name of Degree: **Masters of Engineering (Materials Engineering and Technology)**

Title of Project Paper/Research Report/Dissertation/Thesis ("this Work"):

Masters of Engineering (Materials Engineering and Technology)

Field of Study: **Corrosion**

I do solemnly and sincerely declare that:

(1) I am the sole author/writer of this Work;
(2) This Work is original;
(3) Any use of any work in which copyright exists was done by way of fair dealing and for permitted purposes and any excerpt or extract from, or reference to or reproduction of any copyright work has been disclosed expressly and sufficiently and the title of the Work and its authorship have been acknowledged in this Work;
(4) I do not have any actual knowledge nor do I ought reasonably to know that the making of this work constitutes an infringement of any copyright work;
(5) I hereby assign all and every rights in the copyright to this Work to the University of Malaya ("UM"), who henceforth shall be owner of the copyright in this Work and that any reproduction or use in any form or by any means whatsoever is prohibited without the written consent of UM having been first had and obtained;
(6) I am fully aware that if in the course of making this Work I have infringed any copyright whether intentionally or otherwise, I may be subject to legal action or any other action as may be determined by UM.

Candidate's Signature Date:

Subscribed and solemnly declared before,

Witness's Signature Date:

Name:

Designation:

ABSTRACT

Impress current cathodic protections are common method of protecting steel structure from corrosion attack. The structure are supplied with cathodic current that reduced the corrosion rate. However if the magnitude of current supplied are insufficient, the structure will not be able to be protected and if the current supplied it too high, hydrogen embrittelement may occur. This research studies the effect of cathodic current density on stainless steel by electrochemical testing. A potentiodynamic polarisation test was conducted with stainless steel 316L and 304 in a 3.5% NaCl electrolytic solution. Stainless steel is resistance to corrosion in most atmospheric environment, nonetheless stainless steel is susceptible to pitting corrosion. The effect and the behaviour of stainless steel 316L and 304 under cathodic current are observed in this research as well. The metal surface was analysed by Scanning Electron Microscope and Energy Dispersive X-Ray. The test result indicate that pitting corrosion occur more in 304 stainless steel. On the other hand 316L stainless steel, show a more pitting resistance and slow cathodic rate.

ABSTRAK

Perlindungan katod arus bekasan adalah kaedah yang sering digunakan untuk melindungi struktur keluli daripada karatan. Struktur yang dibekalkan dengan arus katodik akan mengurangkan kadar kakisan. Walau bagaimanapun, sekiranya magnitud arus yang dibekalkan tidak mencukupi, struktur tersebut tidak akan dapat dilindungi. Sekiranya arus yang dibekalkan adalah terlalu tinggi, kerapuhan hidrogen mungkin terjadi. Penyelidikan ini mengkaji kesan ketumpatan arus katodik pada keluli tahan karat menggunakan pengujian elektrokimia. Satu ujian pengutuban potensiodinamik dijalankan dengan keluli tahan karat 316L dan 304 dalam larutan elektrolitik 3.5%NaCl. Keluli tahan karat mempunyai rintangan terhadap kakisan dalam kebanyakan persekitaran atmosferik, tetapi masih terdedah pada kakisan lubang/bopeng. Kesan dan kelakuan keluli tahan karat 316L dan 304 yang dikenakan arus katodik juga diperhatikan dalam penyelidikan ini. Permukaan logam dianalisis menggunakan Mikroskop Imbasan Elektron dan Serakan Tenaga Sinar-X. Keputusan ujian menunjukkan bahawa kakisan lubang berlaku lebih banyak pada keluli tahan karat 304. Manakala keluli tahan karat 316L menunjukkan lebih rintangan terhadap kakisan lubang dan kadar katodik yang perlahan.

ACKNOWLEDGEMENTS

I would like to take this opportunity to convey my earnest and heartfelt gratitude and recognition to each and every one who has supported, motivated, reinforced and assisted me in completing this research project.

Firstly, I would like to take this great opportunity to show my appreciation and gratitude towards my supervisor, Dr. Nazatul Liana Binti Sukiman for her continuous support, guidance and motivation to give in order for me to complete this project with great success and within the given time frame.

Beyond that, I would like to thank Mr. Celestine Gerard for his allocated time and effort in assisting in preparing me samples.

I also would like thank Ms. Cynthia Pinga who has supported me during the journey in completing the project.

Last but not least, my sincerest gratefulness and thanks goes to my beloved family and friends for their reassurance, prayers, inspiration and blessings throughout these academic years. Without their constant guide and support, this achievement would not have been possible for me.

TABLE OF CONTENT

LIST OF FIGURE

LIST OF TABLE

LIST OF SYMBOLS AND ABBREVIATIONS

SEM	-	Scanning Electron Microscopy
EDX	-	Energy Dispersive X-Ray
ICCP	-	Impress Current Cathodic Protection
Na	-	Sodium
Cl	-	Chlorine
PWHT	-	Post Weld Heat Treatment
SSRT	-	Slow Strain Rate
SCC	-	Stress Corrosion Cracking
Mo	-	Molybdenum
SEC	-	Saturated Calomel Electrode

CHAPTER 1 INTRODUCTION

1.1 Stainless steel

Stainless steels are highly corrosion resistance steel and iron based alloy that contain a predominant alloying element of chromium at minimum of 12%. The minimum amount is required to prevent the formation of rust in an ambient atmosphere. Hence the designation stainless came about. The added chromium in the steel creates a passive surface oxide film which protects the underlying metal from corrosion. The oxides forms and heals itself in the presence of oxygen.

The corrosion resistance of stainless steel may also be enhanced by the addition of nickel and molybdenum.

Stainless steel are classified by their constituent of the microstructure such as austenitic, martensitic, ferritic or duplex (consist of both austenitic and ferritic). In addition to the classification is the precipitation-hardenable (PH) stainless steel. This type of stainless steel is based on the type of heat treatment used rather than the microstructure. Austenitic stainless steel are the common stainless steel in the market and they made up the majority of it.

Stainless steel are susceptible to pitting corrosion. Pitting corrosion is a localized type of corrosion which is caused by the break do of the passive oxide layer. Pitting corrosion is an autocatalytic process, where in the vicinity of pit it produce condition that both stimulate and necessary for continuing its anodic reaction in the pit. Researches has indicate that the

addition of molybdenum in austenitic stainless steel increases the resistance of pitting in austenitic stainless steel (ASM, 2000; William Smith, 1993).

Austenitic stainless steel are also venerable to stress corrosion cracking and intregranular corrosion. When austenitic stainless steel is heated to a temperature range of 510-780˚C, they become sensitized to intergranular corrosion (Balasubramaniam, 2010; William Smith, 1993). Intergranular corrosion occurs due to the depletion of chromium adjacent to the grain-boundary. In the temperature range indicated, chromium will be removed from solid solution and will be precipitate as $Cr_{23}C_6$ at the grain boundary. This will occur when carbon content in stainless steel is higher than 0.02%. Since there will be a different polarity present at the grain boundary and the region adjacent to the grain boundary corrosion will occur.

1.2 Problem statement

Cathodic protection is a common method of protecting steel or metal structure that is submerged underground or in an electrolyte via supplying electrons to the structure (Hack, 1999). Supplying electron or cathodic current to the metal structure being protected will eventually bring down the corrosion rate to very low rates (Fontana, 1986; P. R. Roberge, 2000).

There are two method of supplying the electron to the structure being protected, one is known as a sacrificial anode, where a more electropositive metal (reactive metal) are attached to the steel structure (P. R. Roberge, 2000).

The other method is impress current cathodic protection, where current is supplied directly to the structure being protected. Both methods have its benefit and its disadvantages.

In the research we will be focusing more on impress current cathode protection where cathodic current is supplied by a potentiostat.

The fundamental of how cathodic protection works can be easily explained with a pourbaix diagram, in Figure 1.

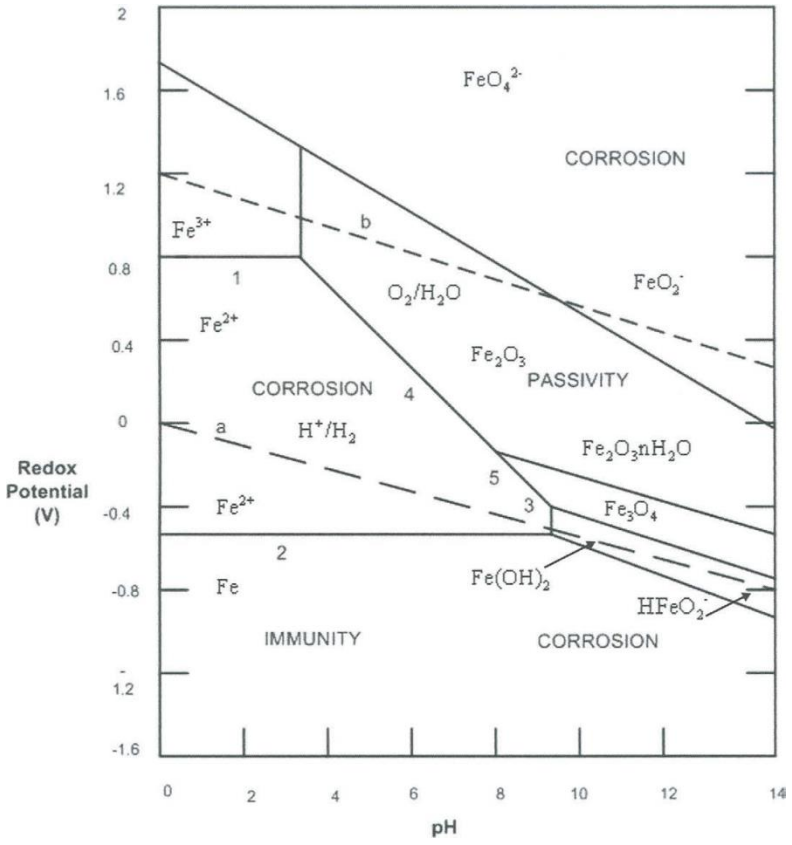

Figure 1 : Potential-pH diagram for iron superimposed with H_2O potential diagram denoted with the dotted line of (a) and (b) (Ahmad, 2006).

Assuming a steel structure is being protected in an electrolyte with pH 6, at zero potential the steel will corrode (anodic reaction) freely. However when a cathodic potential of -0.8V is applied, the corrosion rate will lower down the corrosion rate into the immunity state. Thus the steel will not experience any corrosion.

As good as it sounds this system as a small pit fall. In condition where there is too high cathodic potential (phenomena know as over-potential) supplied to the structure being protected, the rate hydrogen evolution increases. The hydrogen gas released on the structure will induce many negative effects such as hydrogen embrittleement and brittle failure of the structure being protected, which are considered a catastrophic failure with relative to a general corrosion.

The phenomenon of over-potential usually occurs in an impress current cathodic protection system, this is due to the current supplied are powered by an external sourced. Many factors are considered before applying and selecting the voltage for the impress current system. For example factors such as anode placement and distance from the structure being protected, electrolyte resistance, type of coating on the structure, and surface area of the structure being protected.

This research paper is focused on a small aspect on investigating the phenomena of over-potential of stainless steel in 3.5% of sodium chloride solution.

1.3 Research Objective and aims

It is well known that by applying cathodic current to a structure, the corrosion rate is drastically reduced (Barbalat et al., 2013). However in the literature review it will be revealed that in spite of cathodic current applied to structure, in certain cases, it promotes hydrogen embrittlement and pitting corrosion. As such, the project paper seeks to understand the nature of cathodic protection of stainless steel and the occurrence of pitting.

The objective of this research paper is

1. To plot the polarisation curve of stainless steel 316L and 304 in 3.5% NaCl.
    - To investigate the corrosion rate of stainless steel 316L and 304 by electrochemical technique.
2. To identify the severities of pitting corrosion by SEM method on stainless steel 316L and 304 after the electrochemical test.
3. To identify the constituent of the pits after the influence of cathodic polarisation curve via EDX.

1.4 Scope of Studies

The scope of this research is to analyse and understand the effect of the over potential phenomena of cathodic protection in an environment of 3.5% NaCl. It also studies the effects of the pitting formation of both stainless steel 316 and 304 and their resistance to the enviroment. The research primary focuses on the polarization curve to determine the point of corrosion and the rate via electrochemical technique. Scanning Electron Microscope (SEM) and Energy Dispersive Spectroscopy (EDS) are conducted on the corroded surface to identify its properties present on it.

CHAPTER 2 LITERATURE REVIEW

This chapter give a comprehensive view on the cathodic protection, electrochemical measurement of corrosion rate and stainless steel pitting.

2.1 Cathodic Protection

2.1.1 Basic Reaction (Equation)

Cathodic protection is achieved by supplying electrons or cathodic current to the metal structure to be protected. Humphrey Davy used was one of the first to used cathodic protection on British naval ship in 1824 (Ahmad, 2006; Fontana, 1986). The principle of cathodic protection can be explained via electrochemistry. For example a typical metal M in an acidic solution will corrode with the evolution of hydrogen gas as below (P. Roberge, 1999).

Anode : $M \rightarrow M^{n+} + ne^{-}$

Cathode : $2H^{+} + 2e^{-} \rightarrow H_2$

From the above electrochemical equation we understood that the addition of electron or negative current will suppress the degradation of metal M, and with an excess of electron, it might caused the evolution of hydrogen. Therefore using the basic method of electrochemistry, the cathodic protection technology has been developed.

There are two method of applying the cathodic protection principle. The first method is via sacrificial anode and the other is via Impress Current Cathodic Protection (ICCP). For an example a steel structure that wants to be protected is made a cathode by attaching it to an

anode in an electrolyte (which can be water or soil). Cathodic current are applied in the structure, which reduce the corrosion rate thus bring the metal structure closer to an immune state (P. Roberge, 1999).

2.1.2 Sacrificial Anode

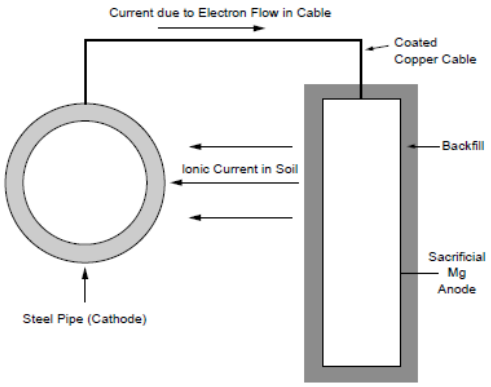

Figure 2 : Sacrificial anode system (P. R. Roberge, 2000)

Sacrificial anode consists of a consumable anode that is relatively more electropositive than the structure being protected. Take for an example the Figure 2, the steel pipe is attached to an sacrificial magnesium anode under the soil. Magnesium anode will corrode which supplies the electron to suppress the corrosion of the steel pipe, thus creating a simple galvanic cell (Crundwell, 2010; P. R. Roberge, 2000).

Anode : $Mg \rightarrow Mg^{2+} + 2e^{-}$

This method of cathodic protection has its advantages such as (P. R. Roberge, 2000).

1. No power source required
2. Low maintenance
3. Unlikely cathodic interference in other structure.

4. Relatively low risk of overprotection

The down falls of this relatively simple system are (Hack, 1999; P. Roberge, 1999).

1. Limited power and current output.

2. Large structure or high resistivity environment may require a large number of anodes.

3. Anodes are required to be replaced frequently under high current system.

4. In some system, anode may increase the weight of the structure if directly attached.

2.1.3 Anode requirements in a sacrificial system

The anode in this system are required to

1. Have a more electropositive or higher position in the E.M.F series relative to the structure being protected.
2. Have enough driving voltage to protect the structure in a particular electrolyte.
3. Have a stable operating potential over a range of current outputs.
4. Have the ability to consistently deliver high capacity of current per unit mass of material consumed, trough out his lifetime.

The common anode that used in this sacrificial anode system are magnesium, zinc and aluminium. Magnesium anodes are preferred than the rest because of its high current output (Ahmad, 2006; Fontana, 1986).

2.1.4 Impress Current Cathodic Protection

The other method is by using an external power supply to protect the structure, which is known as Impress Current Cathodic Protection (ICCP).

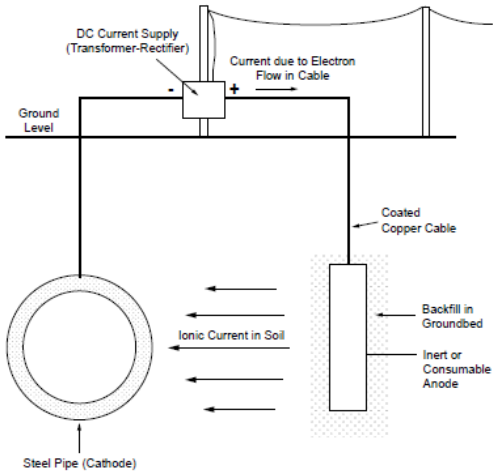

Figure 3: Impress current cathodic protection system (P. R. Roberge, 2000)

ICCP systems are usually used in high-current requirements or high-resistance electrolytes. These systems consist of reactive anodes which are usually made cast iron, graphite or platinum coated graphite. The advantages of the following system are (Balasubramaniam, 2010; Fontana, 1986; Gurrappa, 2005).

1. High power output and high current range
2. Larger protection areas and large structure
3. Lower number of anode in high resistive fluid.
4. Flexibility of current output
5. Applicable in almost any resistivity soil environment

The limitation of this ICCP:

1. External power supply is required and running cost of external power consumption is required.

2. Higher risk of overprotection damage

3. More complex than sacrificial anode system

Blackfill are always used to increase the effective anode size and to lower the resistance of the soils. A good conductivity of anode to the surrounding environment will reduce the anode consumption.

There are many types of anode used in ICCP such as, graphite anode, platinised anode, mixed-metal anode, cast iron or scrap steel.

2.1.5 Type of anodes

Inert anodes are used for impress current cathodic protection because the difference of potential are supplied by an external current supply. Therefore this system does not require an anode that has a higher electronegativity. In impress current cathodic protection inert anode used are (Gurrappa, 2005)

1. Mild steel
2. Cast iron
3. Graphite
4. Platinized titanium anodes
5. Mixmetal oxide anode

The anodes used in the impress current system are required to have long life. Therefore the consumption rates of the anode are important.

The anode use in the impress current system must have few desirable properties such as (Gurrappa, 2005)

1. Good electrical properties
2. Low rate of consumption
3. Low-anode polarization
4. Good mechanical properties

Table 1 : Anode consumption rate and current density (Hack, 1999)

Material	**Anode currents density ($Amps/m^2$)**	**Consumption rate (Kg/Amp.Yr)**
Graphite	2.7-10.7	0.176-4.84
High Silicon Cast Iron	10.7-53.5	0.66-2.42
Platinized anodes	267-1070	6-10Mg./Amp-Yr
Mixed metal oxide	267-1070	Very low

Usually anodes in the impress current system are expected to last for 15-30 years. Therefore anode consumption rate are used to calculate the anode service life (P. R. Roberge, 2000). The anode services life is calculated by using the below

$$\text{Life(Years)} = \frac{\text{Weight (Kg)} \times \text{Utilization}}{\text{AnodeConsumptionRate}\left(\frac{\text{Kg}}{\text{Amp.Yr}}\right) \times \text{I(Amp)}}$$

2.1.6 Other factors System design

Other factors which have to considered before implementation of an impress current cathodic protection system are (Ahmad, 2006; P. R. Roberge, 2000).

1. Corrosion damage under disbanded coating.
2. General current distribution and attenuation (non uniform distribution of cathodic current due to anode placement and irregular distribution of resistance in the electrolyte, distance of anode to the protective structure)
3. Stray current.

2.1.7 Corrosion damage of under disbanded coating

Many cases have been reported in failure of cathodic protection due to disbanded in the coating (Perdomo & Song, 2000; Song & Sridhar, 2008). Buried pipeline are protected with the first layer of defence which are coating on the pipeline, and the second layer will be the cathodic protection. Even after two protection system localized corrosion is identified in the pipeline. The root cause is later identified as disbondment in the coating. Disbondment are a major problem for pipeline coating (Chen, Li, Du, & Cheng, 2009). In the presence of disbondment in the coating, water will enter the disbondment crevice area and create a small electrolyte below the coating. F.M. Song in his study explains that localized crevice corrosion may occur under the disbondment and the cathodic current may not be sufficient to reach the bottom of the crevice and protect the crevice.

2.1.8 General current distribution and attenuation

The anode placement and the number of anode are critical to protect the entire structure. If there is insufficient anode or improper placement (distance from the structure being protected) of anode there will be insufficient current to polarized the entire structure in order to decrease the corrosion rate. Therefore in this situation there will be an irregular current distribution to the structure.

In other situation where impress current may fail is due to the difference of resistance in the electrolyte. Take for an example a buried pipe under the ground which are filled with sandy soil and swamp as the electrolytes.

Table 2 : Resistivity of Different (P. Roberge, 1999)

Electrolytes	**Typical resistivity Ω.cm**
Clay (salt water)	<1000
Clay (fresh water)	<2000
Marsh	1000-3000
Humus	1000-4000
Loam	3000-10,000
Sand	>10,000
Limestone	>20,000
Gravel	>40,000

The current will always take the less resistive path, and therefore more current will pass through the swamp and protect the pipe that particular section and less current will pass through the sandy soil. As in some journals reported that the pH of the electrolyte is very much the current density used to protect the structure (Crundwell, 2010; Metwally, Al-Mandhari, Gastli, & Nadir, 2007). In Table 2 shows the typical resistance of electrolytes or environment. In an actual condition there may be more than one electrolyte present in a system, which makes it harder to predict the current flow and anode placement and also the voltage selection.

Liu Zhiyong studies the significant of non-stable cathodic polarization effect on the SSC of X80 pipeline steel (Zhiyong, Zhongyu, Xiaogang, Cuiwei, & Yunying, 2014). In his finding he concluded that non-stable polarization will enhance both the anodic dissolution and cathodic reaction which results in hydrogen evolution. The non-stable cathodic polarization will firstly discharge the process of the electric double layer and accelerate the mass transport step, which enhance the cathodic reaction of hydrogen evolution. Secondly due to localized anodic dissolution may occur under a non-stable cathodic polarization (Zhiyong et al., 2014).

2.1.9 Stray current

Stray current in fact does not cause much damage to the structure being protected however, it causes damage to the nearby structure. Stray current is current flowing in the electrolyte from an external source like a railways power line (Hack, 1999; P. Roberge, 1999). Stray current tends to enter a buried structure in a particular location and exits in another location. In location where the currents exits the structure, is where the most amount of damage corrosion damage occurs.

2. 2 Impress Current Cathodic Protection Failures

Cathodic protection has it down fall in condition where the structures being protected are excessively negative potential. This will result in hydrogen evolution on the cathode surface which result in hydrogen embrittlement of steel. This will cause the structure to lost its mechanical properties and lead to catastrophic failure (Barbalat et al., 2013; Cheng & Niu, 2007).

ICCP is used in protecting large areas of structure, pipe or concrete underground or in water. One of the important criteria in ICCP is to know how much current to apply on the steel structure to polarise in order to protect it. The protection is applied when the potential is about -850mV with a reference to copper/copper sulphate reference electrode. The application of excessive negative potential leads to hydrogen generation at the protected structure. This will lead to hydrogen embrittlement of the structure, thus reducing the mechanical properties (Cheng & Niu, 2007; B. Huneau & Mendez, 2003; Bertrand Huneau & Mendez, 2006; Lindley & Rudd, 2001).

Seong-Jong Kim conducted a electrochemical studies of cathodic protection of steel in marine structure. He suggested that imposing high levels of impress cathodic current can result in hydrogen embrittlement which can result in failure in high-strength steel, particularly at welds. In his research he investigated the electrochemical effects of post weld heat treatment (PWHT) of high strength steel under slow strain rate (SSRT) test using sacrificial anode in natural sea water. In his finding via SEM fractography, he identified the specimen has transgranular fracture pattern when the potential applied was below -854mV (SCE) and a dimple pattern with ductile fracture when -770~-850mV (SCE) was applied. Therefore, the optimum cathodic protection range between -770-850mV was not causing any hydrogen embrittelement (Kim, Okido, & Moon, 2003).

Study conducted by A.Oni proves that excessive impress-current cathodic protection of dual phase low alloy steel influence the tensile and the yield strength of steel (Oni, 1996). In his experiment he had selected a dual phase steel with a profile of tensile test dimension and immersed it in an electrochemical cell made from trifluoroethene resins with pressure fitting. The specimens were subjected to tensile loads at applied cathodic potentials ranging from -800mV to -1400mV SCE at strain rate of $1.4x10^{-6}$/s until it

fractured. A resilience modulus graph and tensile strength against the applied cathodic protection was plotted. From the graph, it is visible that the tensile strength increased as the cathodic potential increased and decreased rapidly when the applied potential reached -1100mV_{SCE}. It is believed that ICCP resulted in hydrogen generation, thus hydrogen-metal interaction which occurred on the dual phase steel. The hydrogen atom entered into the lattice structure, thus increasing the dislocation within the matrix. Therefore, more stress are required to cause dislocations which explain this increase in strength. He concluded that the interaction resulting from hydrogen entry into the interstitial sites in the lattice structure is due to the application of excessive of cathodic current would have significant influence in the strength behaviour of metal.

In a similar study conducted by Seok-Ki Jang, studied on overpotential phenomena of stainless steel 304, 316, 630 estimated that hydrogen embrittelemt occurred at overpotential of -0.912V, -0.912V, and -1.07V for the respective stainless steel (Jang, Han, & Kim, 2009). In this test he used stainless steel 304, 316 and 630 that are most commonly used as shaft material, structure beam. The Cathodic potential was applied at room temperature using an electrochemical apparatus to plot out a cathodic polarization curve. From the cathodic polarisation curve, information such as activation polarization and concentration polarization for hydrogen gas generation were extracted for each steel sample.

Corrosion potential and current density were determined using Tafel equation and analysis.

$$\Delta V = Ax \ln\left(\frac{i}{i_o}\right)$$

Where V is the overpotential, A is the Tafel slope, and *i* is the current density (A/m^2) and i_o is the exchange current density.

When there was an over potential of -0.912V for 304 stainless steel, there was hydrogen evolution occurred and an evidence of pitting corrosion was evident on the sample. Seok-Ki said there was a possibility that this stainless steel would failure under stress corrosion cracking (SCC) due to pitting caused by the destruction of the chromium oxide passive layer on the steel.

Hydrogen cracking have been attributed to several cases of supermartensitic stainless steel where the source of hydrogen was from the cathodic protection system (Solheim & Solberg, 2013). In an ideal condition, the over potential of the cathode can be controlled by varying the applied current. However in actual environmental condition there are many factors to be considered. For example steel pipelines which are buried under ground that are being protected by impress current method are influenced by many factors such as, conductivity of the soil, aeration, permeability, acidity, humidity, sulfates concentration, chlorides concentration, presence of biological species, stray current, and anode placement in ICCP system (Metwally et al., 2007; Solheim & Solberg, 2013) .

In theory, current for cathodic protection system are determine in consideration of the conductivity of the soil or fluid (V=IR) and the surface area of the structure being protected (Fontana, 1986). Therefore, the current density is an important factor to determine the effectiveness of the protection of the cathodic system. Too much of current density may cause the generation of hydrogen in the cathode, if too little it may cause insufficient protection of the structure. Alternating current has a negative effect on cathodic protection. Study conducted by L.Y Xu on the effect of alternating current on cathodic protection on pipelines, described that the effectiveness of cathodic protection will drop and increased the corrosion rate (L. Y. Xu, Su, & Cheng, 2013).

Z.Y.Liu investigated the relationship of stress corrosion cracking (SCC) , and hydrogen embritelement of X70 pipeline steel under cathodic current in an near-neutral pH of NS4 solution with slow strain rate tensile (SSTT) with various cathodic potential (Liu, Li, & Cheng, 2012a). The X70 steel sample had been subjected the with strain rate of $5x10^{-7}$/s under 1200mV,-1030mV,-925mV,-890mv,-850mV and -750mV until it fractured. The fracture surface was investigate under scanning electron microscope (SEM). While conducting the experiment, a potentiodynamic polarization curves was measured to investigate the electrochemical corrosion behaviour of the steel in the NS_4 solution as the effect of the occurrence of SCC. Z.Y.Liu believed that the applied potential has a large impact on the failure mechanism of the X70 steel. When the applied potential was negative, the steel experience SCC under hydrogen embrittlement mechanism. While the applied potential was more positive, SCC was under anodic dissolution. He concluded that when a steel is in a critical potential range, the steel will be in a non-equilibrium electrochemical state, and anodic dissolution would occur under cathodic polarization potential. This will contribute to the SCC under a combine effect of hydrogen embrittlement and anodic dissolution.

In another study Z.Y.Liu preformed an experiment to understand the occurrence of pitting corrosion of pipeline carbon steel under cathodic protection (Liu, Li, & Cheng, 2012b). In many cases, the SCC of pipeline failure was initiated from pitting corrosion (Dong, Fu, Li, & Cheng, 2008). Z.Y. Lui agrees that the knowledge behind the mechanism of pitting corrosion on a cathodic protected structure is lacking. In his experiment, this pitting corrosion were investigated with two technique which are, the square wave polarization and localized electrochemical impedance spectroscopy measurement. Using the technique above, he found that pitting corrosion could occur at two conditions under

cathodic protection. The first was where the steel experience a potential fluctuation during cathodic protection, thus reversed potential field was generated locally at the surface defect which resulted of localized pitting. The second was where the anodic reaction could take place at localized area to initiate pitting corrosion (Liu et al., 2012b). In an earlier publication Z.Y.Liu, explain that fluctuation polarization generated on the steel electrode would disturbed the local double-charge layer structure (Liu, Li, & Cheng, 2011). Under these circumstances there would be temporary anodic potential field, resulting in a local anodic dissolution to nucleate pits. Local anodic dissolution which results in pits may occur under an unstable cathodic polarization (Liu et al., 2011, 2012a).

Research conducted by M. Javidi on the mechanism of stress corrosion cracking of API 5LX52 steel in near–neutral & high pH environment under cathodic protection, suggested that there are two dominant mechanisms for SCC. When a pipeline is buried underneath the ground, it experience two forms of SCC one is at high pH SCC and near-neutral pH SCC (Cheng & Niu, 2007; M. C. Li & Cheng, 2008). The high pH SCC of carbon steel occur high concentration of biacarbonate at high pH(9-11). This type of SCC have a typical characteristics of intregranular fracture, small amount of lateral corrosion of crack wall and sharp crack tip (Javidi & Bahalaou Horeh, 2014). The rupture of passivation film from the crack tip and dissolution at the grain boundary contributed to anodic dissolution which results to high pH SCC. On the other hand the near-neutral pH SCC are attributed to hydrogen, carbon dioxide which often occur under disbanded of coting of the buried pipelines. This from of SCC is characterise by transgranular crack, with quasi-cleavage and branching of the fracture surface, and lateral corrosion on crack wall (Eslami et al., 2011; D. G. Li, Wang, Chen, & Liang, 2014; Mustapha, Charles, & Hardie, 2012).

Under cathodic protection, the API 5LX52 steel would still fail via stress corrosion cracking mechanisms. The dominating factors that promote these mechanisms are caused by the first the stress experience by the steel and second the applied cathodic current. M. Javidi concluded that the mechanisms of stress corrosion cracking were affected with the applied cathodic potentials. Therefore it is very important to identify the optimum potential for any structure that is protected via impress current cathodic protection.

In a failure analysis journal conducted by University of Calgary, This article include studies of reported case of pipeline failures which covers the effects of cathodic protection on corrosion corrosion fatigue crack, hydrogen embrittlement under and stress corrosion cracking of pipeline in service condition (Shipilov & Le May, 2006). A typical lifetime of a pipeline is determined by the rate of crack propagation. In this literature it pointed out that cathodic protection increases the crack growth rate, and accelerate the crack growth, which is due to hydrogen embrittlement caused by enhance hydrogen uptake in the steel. However there are some date which indicates that the cathodic Protection actually increases banding fatigue strength. This is attributed to the interstitial hydrogen substitution which increase the fatigue limit (Shipilov & Le May, 2006). It is more evident that cathodic current has a significant impact on the mechanical properties of the steel structure being protected and also increases the propagation rate of crack (Oni, 1996; Shipilov & Le May, 2006).

In a similar study conducted by B.Hubeau, on the fatigue behaviour of a high strength steel in vacuum in air and 3.5%NaCl solution under cathodic protection suggested that the cathodic protection condition leads to a reduction of fatigue lives of SE720 steels compared with vacuum (B. Huneau & Mendez, 2003). Both crack initiation points and propagation stage are calculated and observed via SEM. The highest fatigue was measured in vacuum condition, followed by air and the lowest fatigue life was is in NaCl solution.

The number of fatigue cycle recorded in vacuum, air and NaCl with loads of σ_{max} 450MPa are 150,000cycle, ~50,000cycle and ~ 10,000 cycles respectively. The reductions of fatigue life in air are attributed to the gaseous environment, water vapour and hydrogen effect and oxygen playing a role in the crack initiation stage. In the NaCl solution both reduction of crack initiation and propagation stage was observed with reference to vacuum condition. In the NaCl solution hydrogen product are attributed form the cathodic protection. The hydrogen contribute to strong embrittlement of fracture surface which characterized by brittle intergranular crack observed in SEM. Bertrand Huneau also confirms the fact there is a drop fatigue strength of high strength steel in saline solution with cathodic protection, as he conducted the similar study with SE720 steel. He concluded that the hydrogen produced by cathodic protection contributed to the fatigue crack growth rate of the steel. The embrittlement occur via decohesion between prior austenitic grains or martensite laths (Bertrand Huneau & Mendez, 2006).

Wenhe Wang conducted studies of crevice corrosion for buried pipeline with disbonded coating under cathodic protection. He studied the polarization potential,current density, pH value and dissolve oxygen concentration in the crevice (Wang, Wang, Wang, & Yi, 2014). The findings of this investigation suggested that the applied cathodic protection may increases the pH values in the crevice thus increase the rate of corrosion. Cathodic current are unable to reach the bottom of the crevice and reduce the effectiveness of cathodic protection. There is always a potential difference exist between the mouth and in section of the crevice. The normal crevice corrosion mechanisms will take place thus reducing the oxygen concentration and increase the pH values in crevice with time. This was cause by potential drop in the crevice due to solution resistance and current dissipation. High CP is required to achieve corrosion protection at the crevice area due high pH concentration in

the crevice. Higher CP will also increase the risk of hydrogen evolution near the mouth of the crevice (Wang et al., 2014).

In a study conducted by F.Zucchi, on hydrogen embrittlement of duplex stainless steel under cathodic protection in acidic artificial sea water in the presence of sulphide ion, discovered that hydrogen embrittlement are stimulated with high sulphide amount and high voltage of cathodic potential (Zucchi, Grassi, Monticelli, & Trabanelli, 2006). The tests were conducted with different artificial sea water with 0ppm, 1ppm, 10ppm, 30ppm of sulphide ions. Sulphide ion concentration of 1ppm coupled with cathodic potential of -0.9V_{SCE} are sufficient to initiated hydrogen embrittlement in duplex stainless steel. There was a decrease of percentage of elongation of fracture of duplex stainless steel under air condition and under acidic artificial sea water form 1-30ppm sulphide ion condition with increasing voltage. From previous studies it was recorded that the diffusion of hydrogen atoms through the austenitic phase is much slower than through the ferritic phase (Du, Li, Chen, Liang, & Guo, 2008; P. Roberge, 1999; Zakroczymski & Owczarek, 2002). From this investigation, it is understood that increasing current density of a cathodic protection system in an environment that are rich with sulphide ions not necessary will increase the corrosion protection, it might have harm effect on the mechanical properties such as percentage of elongation to the structure (Genel, Demirkol, & Ürgen, 2002; Oni, 1996).

2.3 Stainless Steel

Stainless steel are iron base alloys that contain a minimum of 12% Cr , that forms an invisible and adherent chromium-rich oxide film that prevent it from rust in unpolluted atmosphere. The passive oxide film can be breach or broken down in certain aggressive

environment condition (Ziaei, Mostowfi, Golestani pour, & Ziaei, 2013). Environment condition such as the presence of chloride ions and acidic condition may locally breakdown the passive layer and cause pitting corrosion. Presence of alloying element such as Molybdenum will increase the pitting corrosion resistant of the stainless steel (Pardo et al., 2008a, 2008b; P. R. Roberge, 2000; William Smith, 1993). There are four major types of stainless steels. They are austenitic stainless steel, martensitic stainless steel, ferretic stainless steel, duplex stainless steel and precipitation-hardened stainless steel.

Stainless steel 316L and 304L are austenitic stainless steel with low carbon content and its typically used in food industry, pipeline industry (Smith, 1993) . In general the austenitic stainless steel is resistance to all industrial atmosphere and some acid media. Stainless steel 316L, has a high corrosion resistance, high strength and high durability and it are used in many marine application (Cai et al., 2010). However they are susceptible to intergranular corrosion, stress corrosion cracking and localized corrosion such as pitting corrosion and crevice corrosion (Cai et al., 2010; Jin, Xie, & Tian, 2012). Intergranular corrosion of stainless steel results from microstructure changes, where chromium carbides (Cr_3C_6) precipitated at the grain boundary and cause a depletion of chromium adjacent to it. The difference in chemistry from the precipitates and the adjacent induce corrosion to occur (Matula et al., 2001). Most of the corrosion attack on stainless steel starts with small pits formation and grows via different corrosion mechanisms (Roffey & Davies, 2014; Ziaei et al., 2013).

S.S Xin conducted an electrochemical corrosion characteristic of 316L stainless steel in hot concentrated artificial seawater. In this investigation S.S Xin, immersed 316L in artificial seawater having a pH value of 8.2 at 72˚C for 3200hr (Xin & Li, 2014). Form this immersion of 316L stainless steel 3 stages are observed, passive stage, transient stage and

stable pitting stage. In the passive stage, it involves the dissolution of passive film and the deposition of salts. At this stage the corrosion potential increase quickly and decrease gradually at a steady corrosion state due to the salt formation. In the second stage (transient), the corrosion rate decrease drastically due to the initiation and formation of pitting corrosion. At the third stage (pitting), the active pits grow which are accompanied with new formation of pits. Pitting corrosion attacks begin at about 1150hr of immersion, with stage 1 with deposition of salts. The maximum pit depth was measured at 38μm after a year of immersion. From this experiment S.S Xin concluded that 316L stainless steel has a good pitting resistance to hot artificial seawater.

In another studies Congmin Xu, suggested that the pitting resistance of 316L stainless steel will decrease in the media of sulphate-reducing and iron-oxidizing bacteria. The corrosion potential, pitting potential and polarization resistance of stainless steel 316L will decrease in the presence of these bacteria, thus accelerating the pitting corrosion (C. Xu, Zhang, Cheng, & Zhu, 2008).

However it is well known that corrosion resistance or to be precise pitting resistance of stainless steel can be improved by the addition on molybdenum (Mo). Addition of molybdenum into stainless steel increases the general corrosion resistance of the steel. Molybdenum modifies the passive film composition and the active dissolution by formation of insoluble oxides (Pardo et al., 2008a, 2008b).

Stainless steel 304 has a slightly lower levels of chromium compare to stainless steel 316l, it has an average corrosion resistance to sulfuric acid solution. In comparative study on corrosion behaviour of stainless steel 304 in sulfamic (NH_2SO_3H) and sulfuric acid, revealed that the corrosion rate are higher in sulfuric acid than in sulfamic acid in all condition (Hermas & Morad, 2008).

2.4 Pitting Corrosion

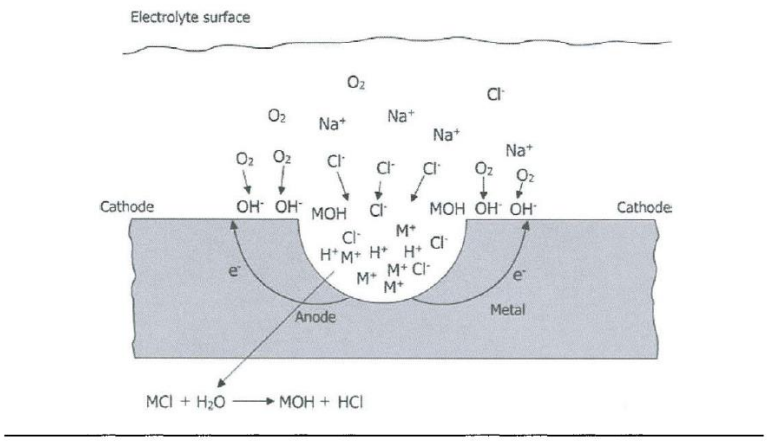

Figure 4: Pitting corrosion mechanisms (Ahmad, 2006)

Pitting mechanisms in steel, is shown in the stage below

Stage 1: $Fe \rightarrow Fe^{2+} + 2e^{-}$ (anodic)

Stage 2: $O_2 + 2H_2O + 4e^{-} \rightarrow 4OH^{-}$ (cathodic)

Stage 3: $Fe^{+}Cl^{-} + H_2O \rightarrow FeOH + H^{+} + Cl^{-}$

A pitting corrosion mechanism occurs in three stages. The first stage is the dissolution of the iron. The continual dissolution of positively charge iron ions in the pits are electrostatically balanced by cations such as Cl^{-}, OH^{-} ions. OH^{-} ions migrate in slower rate, compare to Cl^{-} ions which are small (Loto, 2013). The three stages that is the hydrolysis reaction, where iron chlorides are broke down. That results the formation of iron hydroxide and hydrochloric acid. The presence of H^{+} ions and chloride content prevents repassivation and decreases the pH value in the pits (Ahmad, 2006). This process is an autocatalytic an it increases with time resulting in more metal dissolution.

Pitting corrosion are usually caused by the damage of the passive oxide layer of stainless steel that expose the stainless steel to aggressive environment. R.T Toto explains the passive oxide film should be view as a dynamic film (Loto, 2013). The passive film break down and pit initiation are categorized into 3 main mechanisms. That is film penetration, film breaking and adsorption. In the penetration stage, migration of Cl^- ion occurs from the electrolyte through the passive layer to the oxide-metal interface by the influence of high electrical potential. The film breaking mechanisms initiated with cracks, inclusion, or defect on the passive layer will slowly expose small areas metal surface to the electrolyte the initiated pits (Ahmad, 2006; Loto, 2013). In adsorption mechanism, there will be an increase of transfer cations from the passive film to the electrolyte. This process will result in the thinning and the removal of the passive layer (Loto, 2013).

2.5 Polarization Curve for stainless steel

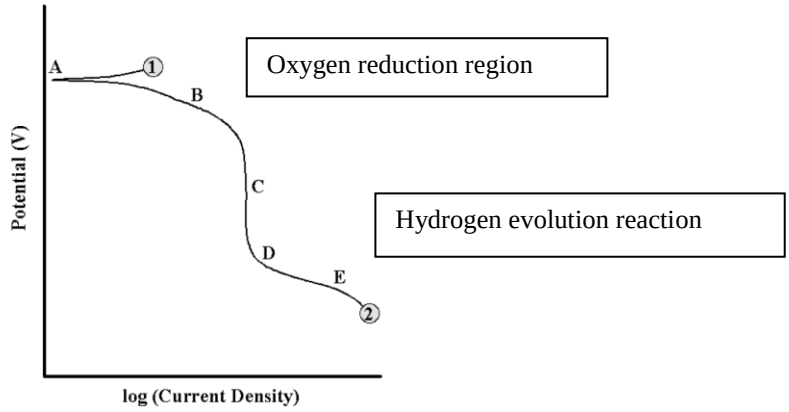

Figure 5: A theoretical cathodic polarisation scan (Enos, 2008)

A cathodic polarisation scans begin at point 1 and ends at point 2. Point A is the open circuit potential which is the sum of both anodic and cathodic reaction occurring on the electrode surface are zero. Regions B represent the oxygen reduction reaction and its

dependent on the pH and dissolve oxygen concentration in the solution. As the applied potential decrease, there will be no change in reaction at region C, until the potential becomes sufficiently negative for cathodic reaction to initiated. At point D to E, there will be a reduction of water, as such hydrogen evolution reaction occurs. Current density may increases when the is a sufficient driving force (Enos, 2008).

The anodic polarization curve, is an important graph which provide information on the corrosion rate and the active-to-passive transition (Alvarez, Bautista, & Velasco, 2013). S.M. Alvarez conducted a study, on anodic dissolution on various type of austenitic stainless steel in acid medium. He was investigating the influence of induce martensite microstructure on the corrosion behaviour of stainless steel. The electrochemical test was conducted by using a Potentiostat, 2M H_2SO_4 + 0.5M HCL solution as an electrolyte, and saturated calomel electrode (SCE) as a reference electrode, and stainless steel mesh as a counter-electrode.

From his result (Figure 6), it is understood that the maximum corrosion rate occur at E= -200mV. The corrosion rate continues to decrease with increasing E (>-200mV) for all the stainless steel until it reaches a passive state.

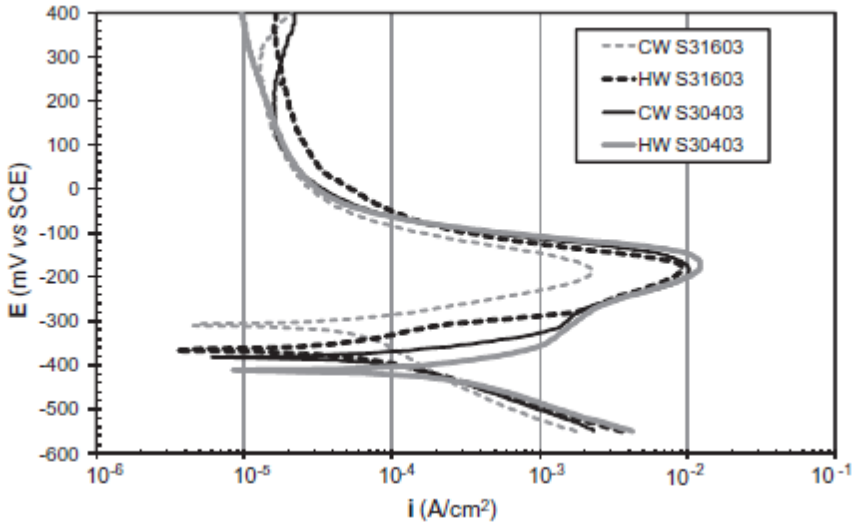

Figure 6 : Anodic polarization curves of the four studied austenitic stainless steel bars in 0.5M HCl + 2M H_2SO_4 (Alvarez et al., 2013).

S.M. Alvarez concluded that the induce martensite in austenitic stainless steel strongly influence the anodic dissolution and the corrosion resistance of it. However the influences of the corrosion behaviour are very much dependent on the distribution and the amount of the martensite in the stainless steel.

The anodic polarization curves also provide the critical voltage that are needed to be avoided to prevent hydrogen evolution. In the case of previous journal (Genel et al., 2002; Bertrand Huneau & Mendez, 2006; Kim et al., 2003; Oni, 1996) on the influence of cathodic current on the mechanical properties, Kenan Genel studied the effect of cathodic polarization on corrosion fatigue behavior of ion nitride AISI 4140 steel (Genel et al., 2002). He obtained the anodic polarization curve for both nitride and non nitride AISI 4140 steel. Below in figure 7 was his result of the anodic polarization curve.

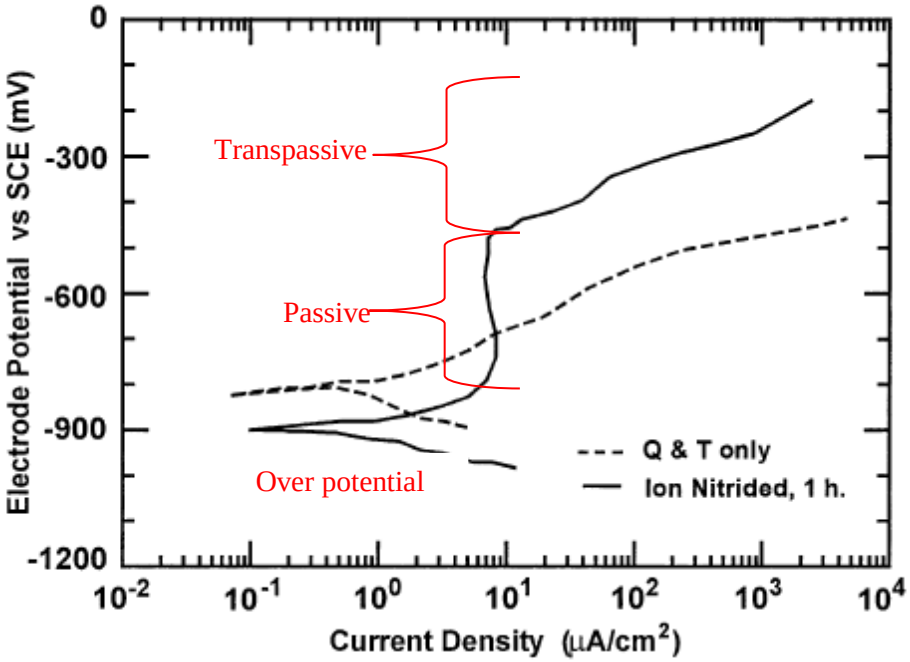

Figure 7 : Polarisation curves of AISI 4140 steel in deaerated 3% NaCl solution for tempered and ion nitrided specimens.

The sample that is not nitride (quenched and tempered), shows no visible active-to-passive transition, unlike the nitrided sample. The non-nitrided sample continues to corrode with higher current density with increase of electrode potential.

On the other hand the nitrided sample, show a decrease in current density when the electrode potential was about -900mV. At this stage the vertical line in the graph represents the passivation, where the corrosion current density drop. Increasing the electrode potential above -600mV, destroy the passive film and thus increase the corrosion rate. Genel selected three cathodic potentials which are from the passive, cathodic and the over-chatodic region of anodic curve to conduct the fatigue test in 3%NaCl. Potential -750mV which lies within the passive line, -1080mV potential that is within the cathodic line and -1500mV the over-cahtodic region.

The result of the fatigue show that the -750mV was insufficient to protect the steel, thus corrosion occurred and the fatigue strength reduced. At -1080mV its showed the best result of corrosion protection and increase in fatigue strength. On the negative side potential of -1500mV displays hydrogen evolution during the test, and a drastic decrease in fatigue strength.

Put it into perspective, if an impress current cathodic protection is applied on AISI 4140 steel with a potential of -1500nV in a 3%NaCl environment it would eventually fail via hydrogen embrittlement. However, if there is a change in the electrolyte concentration in the soil, or change in distance of anode placement this current may not cause hydrogen evolution on the steel. Therefore it is curtail to identify variable in the environment to select the optimum potential.

L. Freire had conducted a study of electrochemical behaviour of stainless steel 304 in different solutions of pH (pH9, pH10, pH13) with the presence of chloride ions (Freire, Carmezim, Ferreira, & Montemor, 2011). His aim was to study the passivation and passivation breakdown of stainless steel 304 in different electrolyte. Results show that pH has a large impact in the formation of film resistance, charge transfer and thus the anodic dissolution.

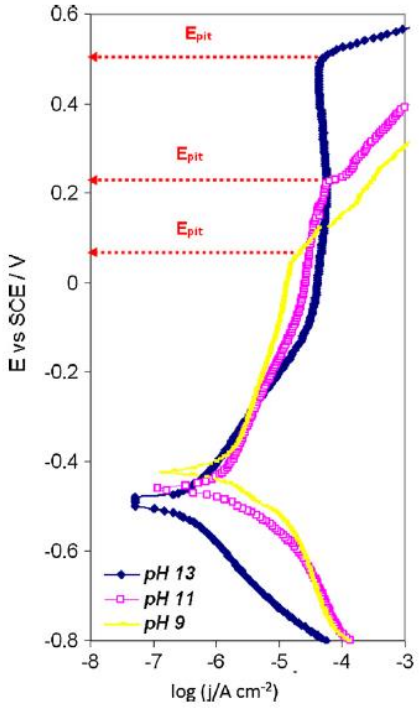

Figure 8: D.C potentiodynamic polarization plots obtained in the anodic direction for AISI 304 in NaOH+KOH solutions at different pH (13,11 and 9) contaminated with 10% NaCl (scan rate=10mVs−1).

For the Figure 8 obtain from L. Freire work, it was observed that as the solution become less alkaline, there was a shift of corrosion potential to be in a more positive potential and the pitting potential towards more a cathodic state. Pitting process was initiated at a lower potential for low pH solution, and an increasing trend of pitting potential as the pH increases. L. Freire concluded that in the presence of chloride ions, the surface films formed a higher resistance and slightly lower charge transfer resistance, thus the drop in pH makes the surface more sensitive to chloride pitting attacks.

2.6 New technology for cathodic protection

In recent times there a major improvement in corrosion prevention for metal and steel. It is a common to reduce corrosion attack by a typical protection of organic coating and the common sacrificial anode and impress current cathodic protection as discussed previously (Lei, Liu, Zhou, Feng, & Du, 2013). However the protection method such as sacrificial anode and ICCP, has a limited life time due to the anode deterioration. Ynan and Tsujikawa suggested a new concept of photogenerated cathodic protection layer (Yuan & Tsujikawa, 1995). Later in the industry Park, was able to developed a method using a semiconductor TiO_2-based photoelectrochemical to be a photoanode (subsutitue for sacrificial anode) for corrosion prevention (Park, Kim, & Choi, 2001, 2002). Now TiO_2 films are used as photoanodes for cathodic protection of metals.

In a recent studies conducted by Caixiz Lei, on photo generated cathodic protection of stainless steel by liquid phase deposited sodium polyacrylate/TiO_2 hybrid films suggested that addition of sodium polyacrylate improve the photochemical respond of TiO_2 (Lei et al., 2013). In his research he prepared sodium polyacrylate/TiO_2 hybrid films by liquid phase deposited method. The hybrid films were co-doped with elements of nitrogen and fluorine which stimulate the respond to visible light. This new hybrid film could provide sufficient negative photopotential for the cathodic protection of 304 stainless steel.

CHAPTER 3 METHODOLOGY

3.1 Material

3.1.1 Sample and solution preparation

Stainless steel 316L and 304 sourced from a local supplier and was manufactured in Korea and India respectively. The sample was cut into 10mm thickness and was mounted. After the mounting, a small section was drilled and a copper wire was attached to the stainless steel sample.

Austenitic stainless steel are generally non hardenable via heat treatment and therefore are used in annealed condition. Below are the typical chemical compositions of both the stainless steel

Table 3 : Chemical composition of stainless steel 316L and 304

Stainless Steel /Elements	C%	Mn%	Si%	Cr%	Ni%	Mo%	N%	S%	P%
316L	0.03	2.00	0.75	16.0-18.0	10.0-14.0	2.0-3.0	0.10	0.030	0.045
304	0.08	2.00	0.75	18.0-20.0	8.0-12.0	-	0.10	0.030	0.045

Stainless steel 316L and 304 that were already cut to size of 15mm diameter and 10mm length were mounted and abraded with 600, 1000, 1200, 2000-grit silicon carbide paper in order to remove scratches and provide a smooth surface. Samples were then washed by distilled water and degreased with acetone. Tow of stainless steel 316L and 304 were polished up to 1µm with diamond past that was used as a reference sample for SEM testing and microstructure analysis. The electrolyte 3.5%NaCl was prepared by dissolving 35g of NaCl in 1000ml of distilled water.

3.2 Hardness test

3.2.1 Micro Vickers Hardness Tester

Figure 9: Vickers hardness tester

Zwick Roell Indentec Micro-Vickers hardness tester with 0.5Kg as load were used to determine the hardness of the stainless steel sampled used. 5 indentations were performed on the sample to obtain the average reading from both the steel sample. The sample was grind up to 2000 mesh sand paper before performing the Vickers hardness test.

3.3 Metallography

Stainless steel 316L and 304 samples, that were grounded up to 2000 mesh was later polish with 1µm diamond paste. The sample was later clean via acetone and etched with Kalling-2 etchant. The microstructure was observed via optical microscope.

3.4 Electrochemical Test

3.4.1 Potentiodynamic Polarisation Test

Figure 10 : Potentiostat

Potentiodynamic polarisation tests were performed using a standard theee-electrode flat-cell and under the control of GAMARY software. A saturated calomel electrode was used as a reference and platinum mesh was used as a counter electrode. After corrosion test was completed, current densities, corrosion potential were estimated by linear fit and tafel extrapolation was conducted to estimate corrosion potential.

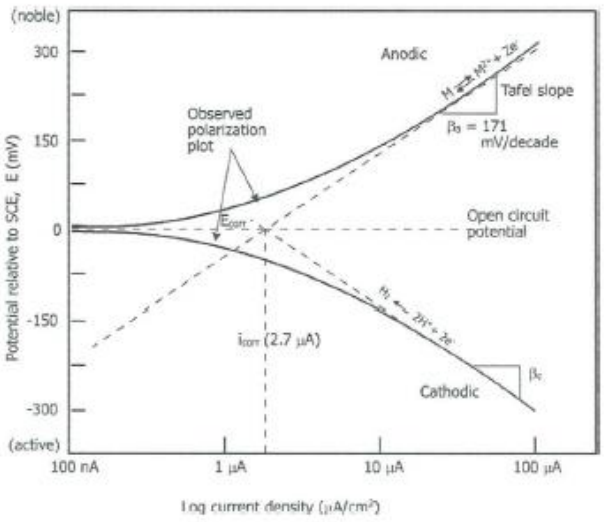

Figure 11: Hypobolic Tafel plot

In order to obtain the E_{Coor} and i_{Coor}, Tafel plot were used. The Tafel plot is a useful method to obtain instant measurement of corrosion current density. It is obtained by plotting the logarithms of current (anodic and cathodic) vs potential and extrapolating the currents in the two Tafel regions. i_{Coor} is obtain at the intersection between the anodic and cathodic reaction where the rate of oxidation and reduction are equal. A slop that exhibit Tafel behaviour (linear or semi-logarithmic) is extrapolated from 50 to 100mV from E_{Coor} from both anodic and cathodic reaction in Figure 11.

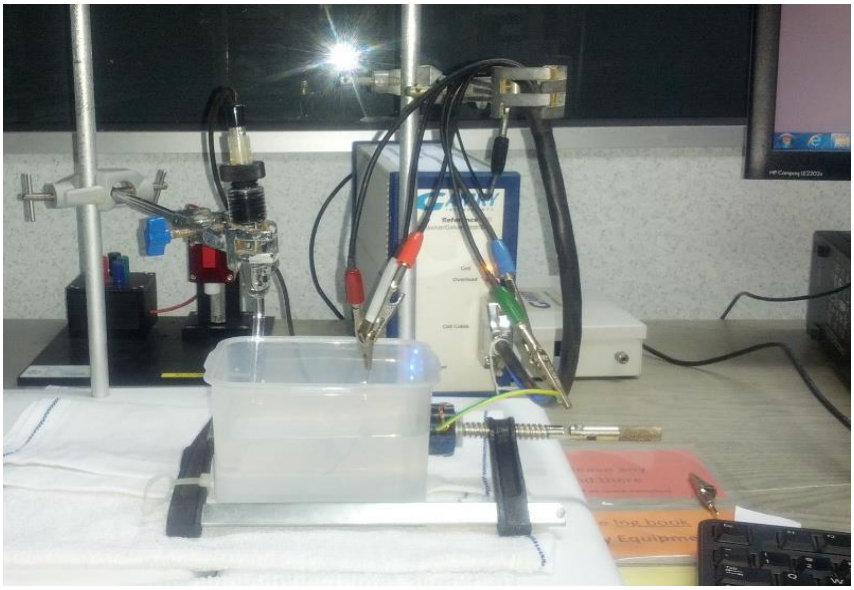

Figure 12 : Apparatus set up

Potentiodynamic polarisation (PDP) test were perform using the set up above. The electrolyte used in the test was 3.5%NaCl. The scan rate of the experiment was selected at 1mV/second of potentiodynamic polarisation test. The initial and the end voltage are inserted into the software before conducting the polarisation test. Once the test is complete the sample is removed and store in an air tight container for SEM testing. First the test is conducted using the first sample of stainless steel 316L and then repeated using the second sample of 316L and followed by 304.

3.5 Surface Characterisation

3.5.1 SEM and EDX

Figure 13: PHENOM Table Top SEM

PHENOM ProX table top SEM with built in EDX features at Faculty of Engineering UM was used to identify and observe the severity of the pitting. The images were observed using back scattered electron (BSE) and the elements in the pits were analysed via energy-dispersive X-ray (EDX). Stainless steel test sample after electrochemical testing were analysed using the SEM and EDX above.

The polish sample of both stainless steel 316L and 304 were analysed via SEM to determinate the surface condition as for reference purposes. The stainless steel sample that underwent the electrochemical test, were then analyzed in SEM and EDX. The same magnifications were chosen to differentiate the intensity of pitting between both stainless 316L and 304. Several pitting spot were analysed via EDX to identify its principle elemental constituent.

The test data and the experimental result that were obtained was complied and analysed according to determine the effect of cathodic current density on the criticality of pitting using potentiodynamic test and SEM.

CHAPTER 4 RESULT AND DISCUSSION

4.1 Hardness

Table 4 : Average hardness measurement of stainless steel 316L and 304

Material/ Hardness reading	316L stainless steel	304 stainless steel
1st	161HV	235HV
2nd	178HV	275HV
3rd	181HV	256HV
4th	180HV	239HV
5th	178HV	248HV
Average Vickers hardness	175HV	251HV

Stainless steel 316L has a lower hardness with respect to stainless steel 304 in Table 4. This is because stainless steel 304 has a higher carbon content that stainless steel 316L. The Vickers hardness of 316L and 304 stainless steel are in agreement with the hardness value reported by (Muthukumaran, Selladurai, Nandhakumar, & Senthilkumar, 2010)and (Milad, Zreiba, Elhalouani, & Baradai, 2008).

4.2 Metallography

4.2.1 Microstructure of Stainless steel 316L

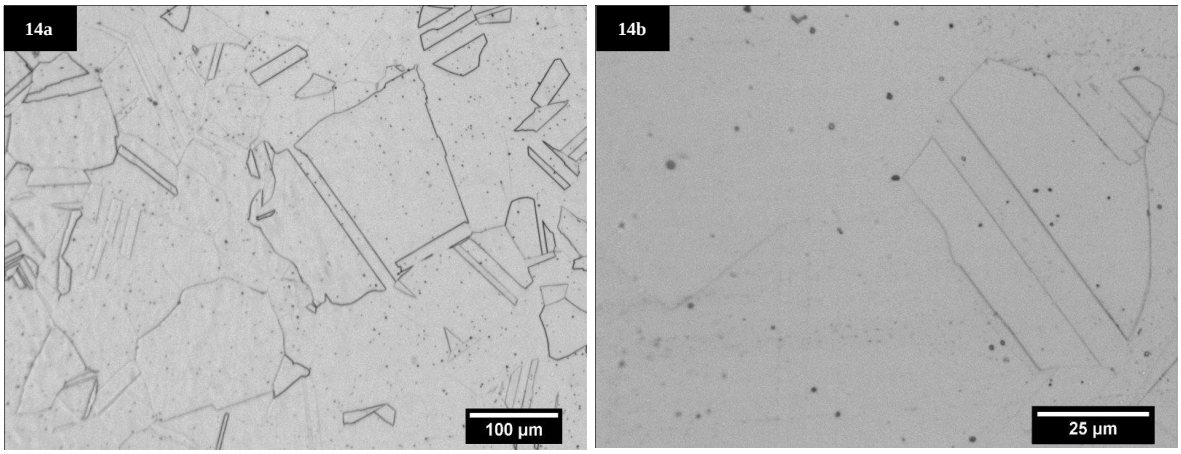

Figure 14a : Solution anneled structure of 316L at 100X etched with Kalling's No. 2. Figure 14b 500X view on the austenitic grain.

4.2.2 Microstructure of Stainless steel 304

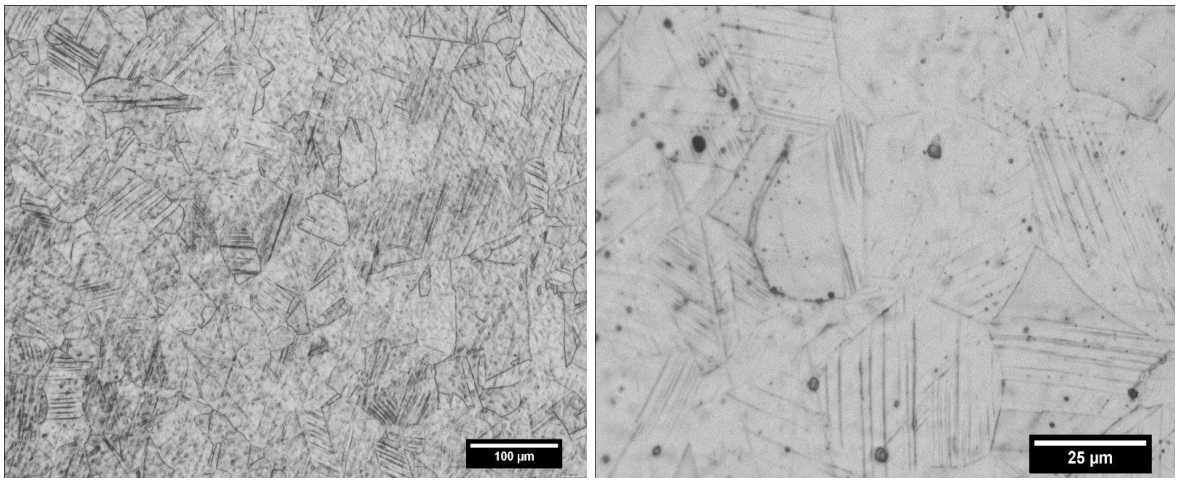

Figure 15a : Stianless steel 304, 100X etched with Kalling's No. 2. Figure15b 500X, view on the induce maretensitic in austenitic grains.

The microstructure of stainless steel 316L in solution anneled consist of normal austenitic microstructure (Figure 14a and 14b). In stainless steel 304 it was observed to have been some strain-induced martensite structure. This explains the relatively higher hardness of

304 relative to 316L recorded in Table 4. There must have been some amount of cold work involved in stainless steel 304 that has caused induced mastensite structure.

4.3 Electrochemical test

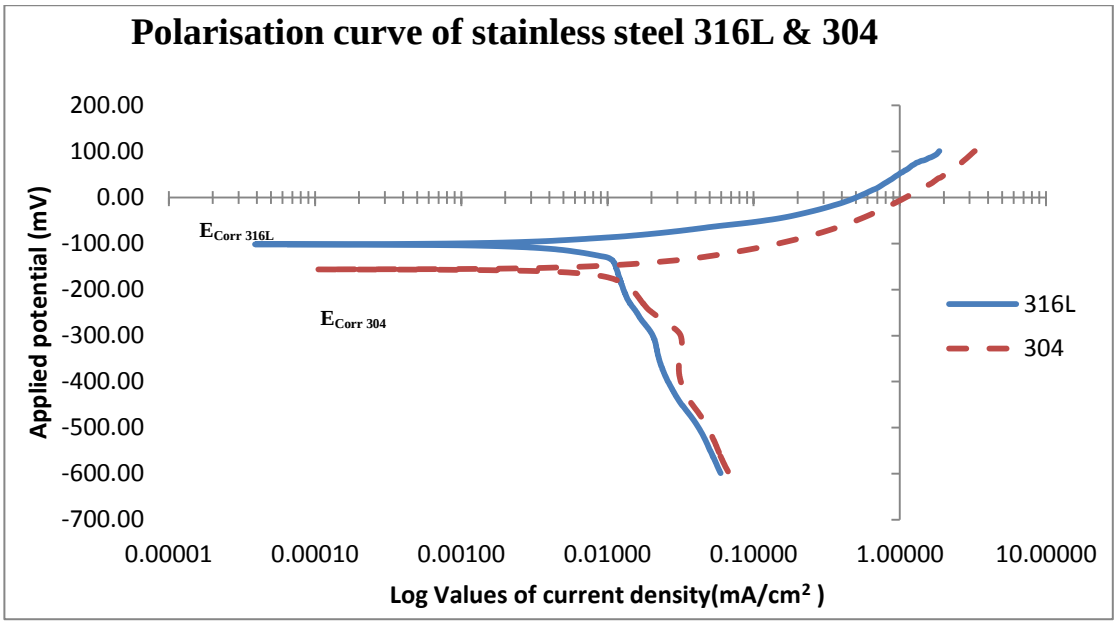

Figure 16 : Polarisation curve of stainless steel 316L and 304.

Figure 16 display the result of the potentiodynamic test for both stainless steel 316L and 304 in a graph. From the Figure 16, it is very much visible that stainless steel 316L has a higher corrosion potential E_{Coor} than stainless steel 304.

4.4 Tafel plots analysis

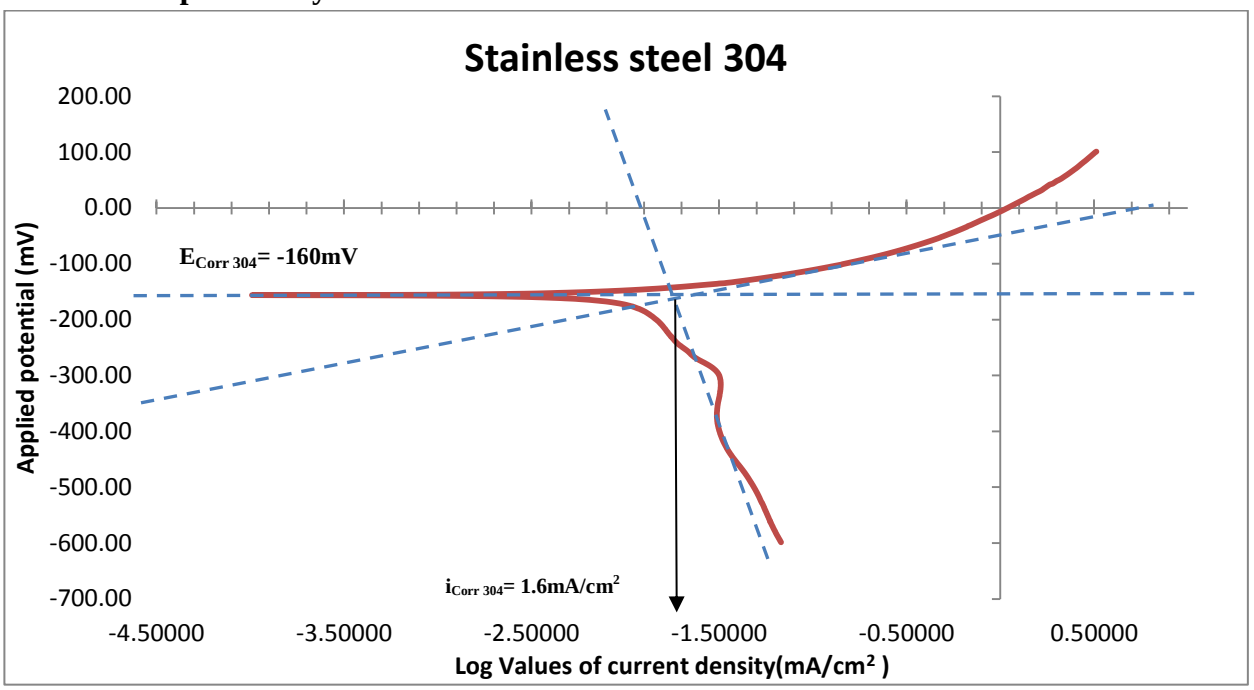

Figure 17 : Tafel plot for stainless steel 304

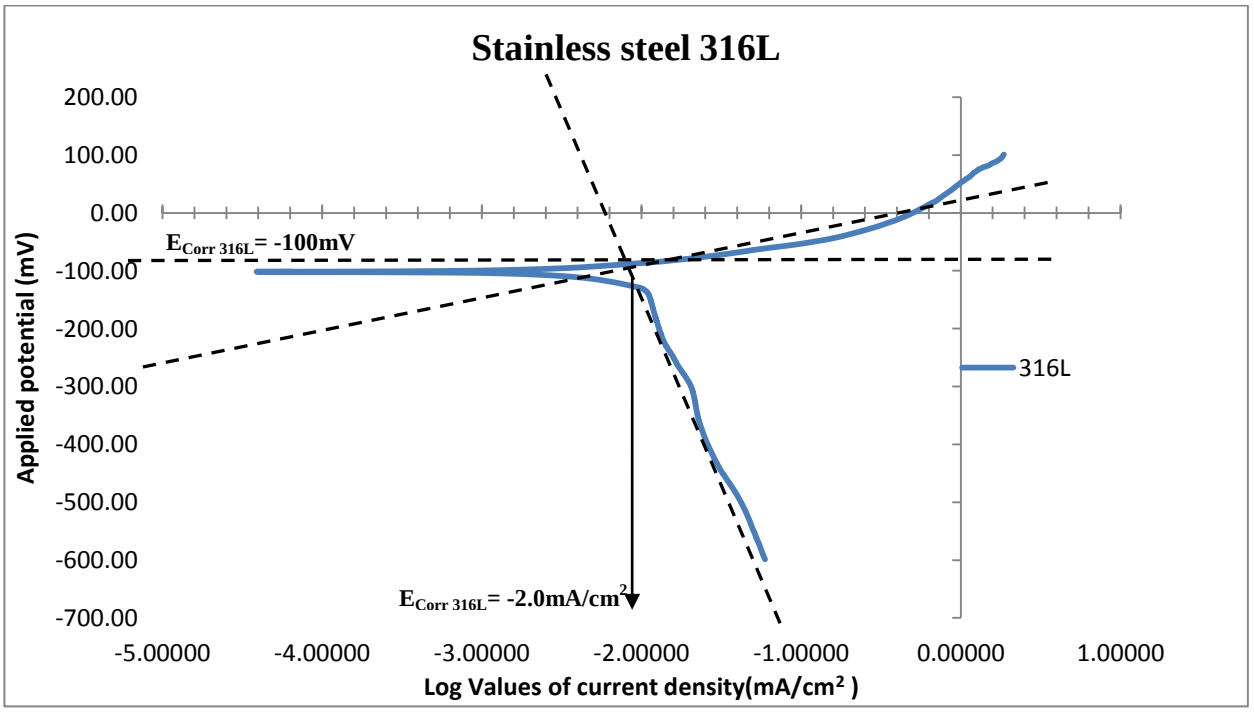

Figure 18 : Tafel plot for stainless steel 316L

Table 5 : Electrochemical result

Material	**E_{Corr} Corrosion potential/mV**	**I_{Corr} Corrosion current density/(mA/cm^2)**
304	-160	1.6
316L	-100	2.0

Figure 17 and Figure 18, is the extropoltion of the tafel method to obtain the E_{Corr} and I_{Corr} value. The Potentiodynamic of both stainless steel 316L and 304 conducted at 25˚C in 3.5% NaCl electrolyte and scanning rate of 1mV/s. The result in table 5 indicates that 316L has a higher E_{Corr} with reference to 304, since the inflection point of 316L are above 304. The higher E_{Corr} of 316L may be explained by the higher chromium and nickel compared to 304. In general higher chromium and nickel improve the corrosion resistance of stainless steel.

As discussed in the literature review on David G Enos work, on potentiodynamic polarisation scan, a typical cathodic polarisation curve will consist of two stages, which the oxygen reduction stage and the hydrogen evolution stages (Enos, 2008). Form the result in figure 16, it is observed the electrode potential for hydrogen embrittlement has not been achieved, thus the dominant reaction is the reduction of oxygen. Base on the microstrcutre of stainless steel 304, it was identified to have small amount of strain induce martensite. Having martensite in the microstructure would very much lower down the corrosion potential as it have reported by Alvarez (Alvarez et al., 2013).

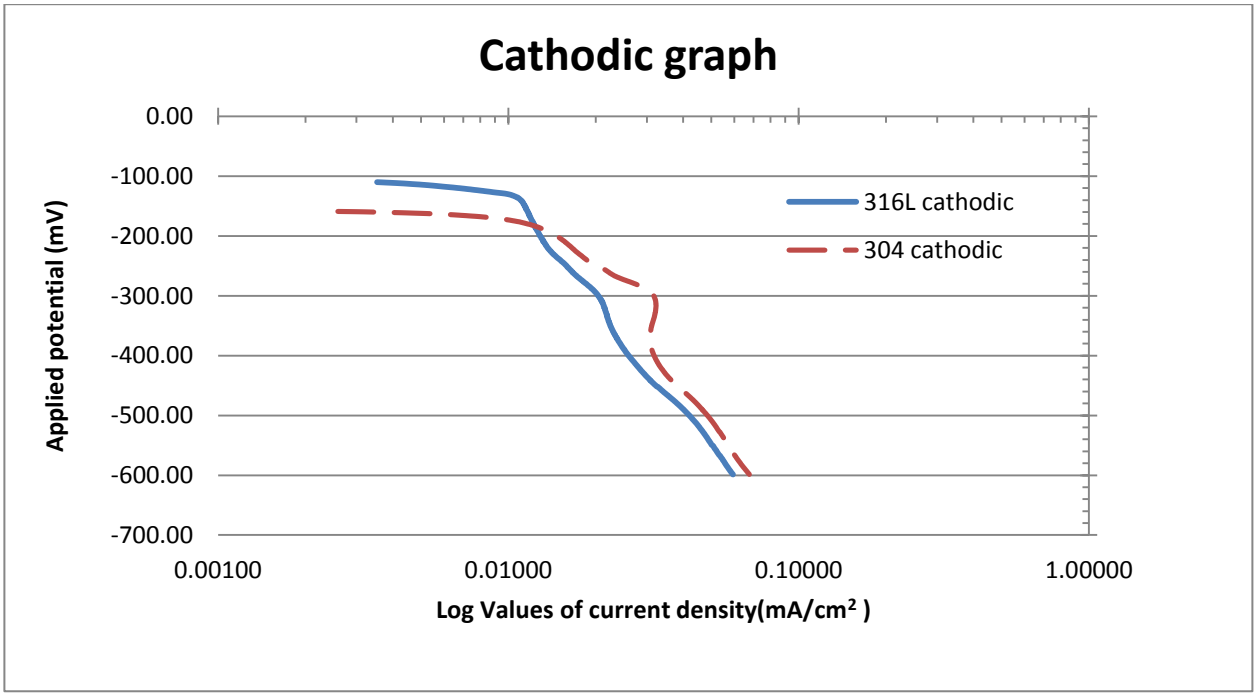

Figure 19 : Cathodic graph and tafel extrapolation

The cathodic graph in Figure 19 shows that stainless steel 304 has a faster and a lower cathodic reaction rate compared to 316L. This explains the finding in SEM (Figure 23a and 23b), where there were more pitting corrosion observed in 304 compared to stainless steel 316L.

4.5 SEM

4.5.1 Stainless steel 304 and 316L polish surface

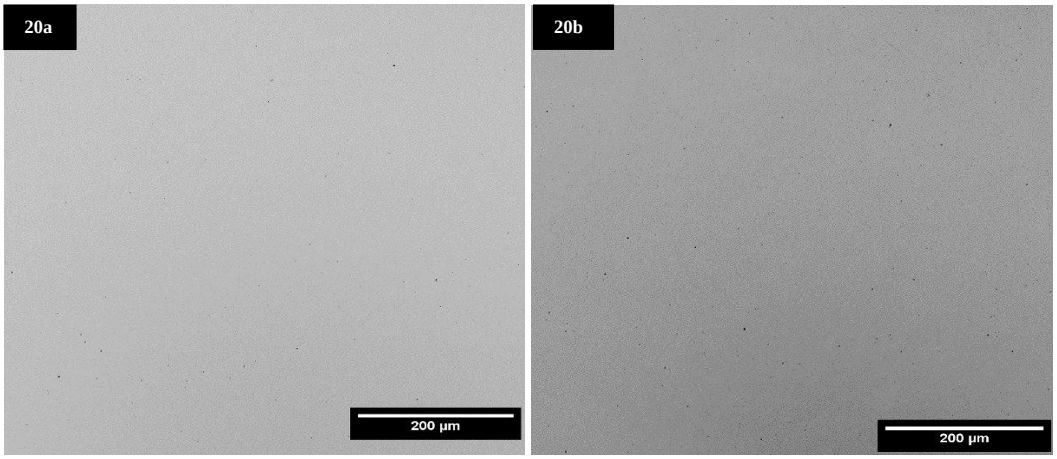

Figure 20a : Stainless steel 304 at 400X, Figure 20b: stainless steel 316L at 400X

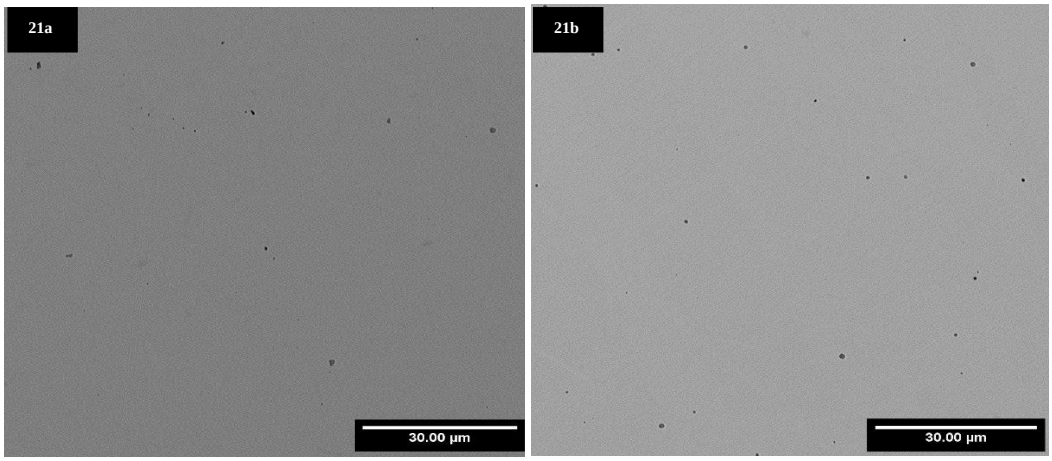

Figure 21a : Stainless steel 304 at 2700X, Figure 21b: stainless steel 316L at 2700X

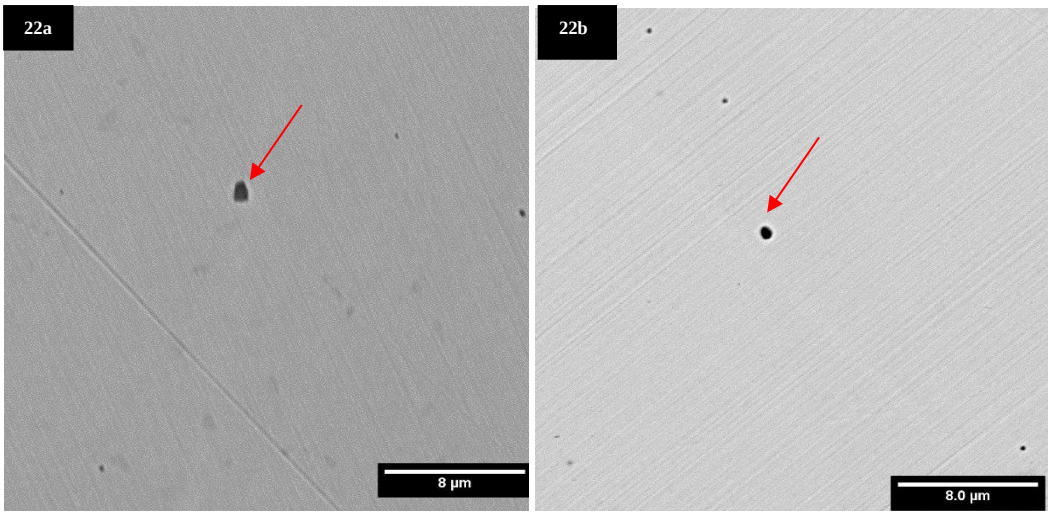

Figure 22a : Stainless steel 304 at 9100X, Figure 22b: stainless steel 316L at 9100X

A polish 304 was analysed using SEM, the result in Figure 21 and Figure 22 indicate several formation of pits in different magnification. This pits are not a result of corrosion, however are result of the polishing and the polishing method. Both the sample were polish up to 3µ and then up to 1µm with diamond paste. The polishing was done in an automated polish machine that polishes at high rpm. Usually soft materials are polish with low rmp and with low pressure. If pits are still present, its recommended to polish for short periods and to clean it between.

4.5.2 Stainless steel 304 and 316L after polarisation test

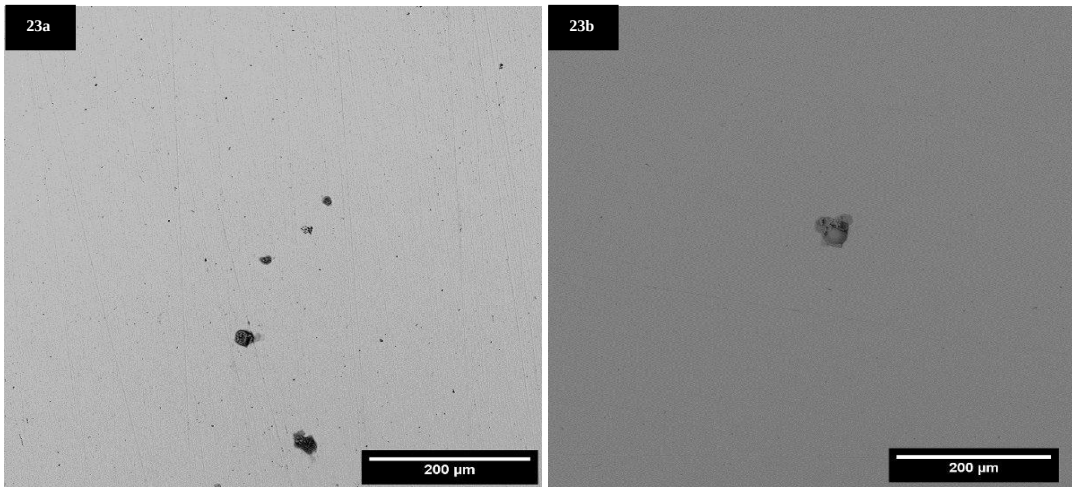

Figure 23a : Stainless steel 304 at 400X several pits were identify , Figure 23b: stainless steel 316L at 400X, few pits were identify.

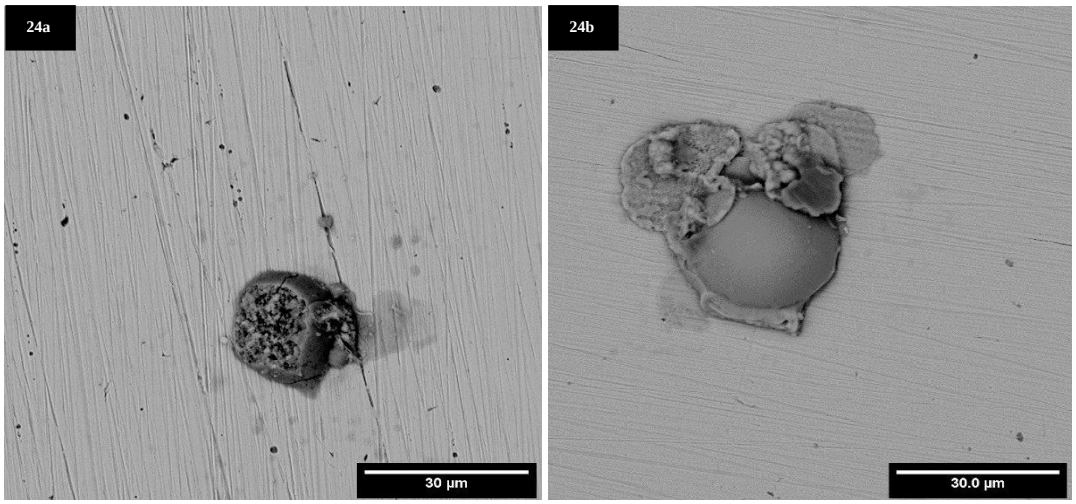

Figure 24a: 2700X view on stainless steel 304 pits, Figure 24b: 2700X view on stainless steel 316L pits.

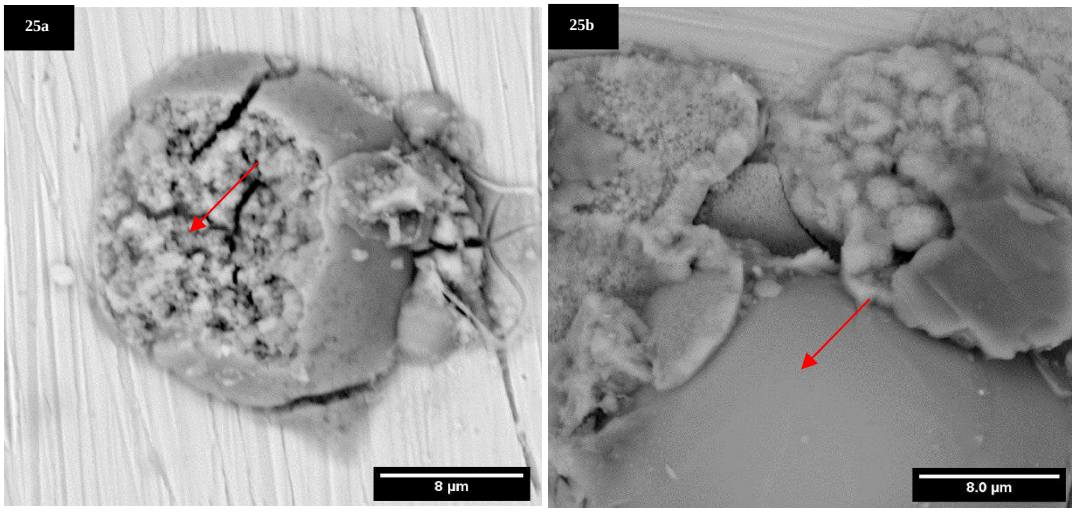

Figure 25a : 9100X view no stainless steel 304 pit, Figure 25b: 9100X on stainless steel 316L pits.

For the SEM result at 410X, it was observed that there were more pits formation on the 304 stainless steel comparative to 316L (Figure 23a and 23b). This may be due to the addition of molybdenum element in 316L stainless steel increases the pitting resistance. The presence of molybdenum in the stainless steel influences the passive chromium oxide film of the steel (Pardo et al., 2008a). Molybdenum were present in the passive layer as molybdates (MoO_4^{2-}) ions, which are on the top of the material surface. This molybdates acted as a barrier against the electrochemical attacks.

4.6 EDX at Corroded Area

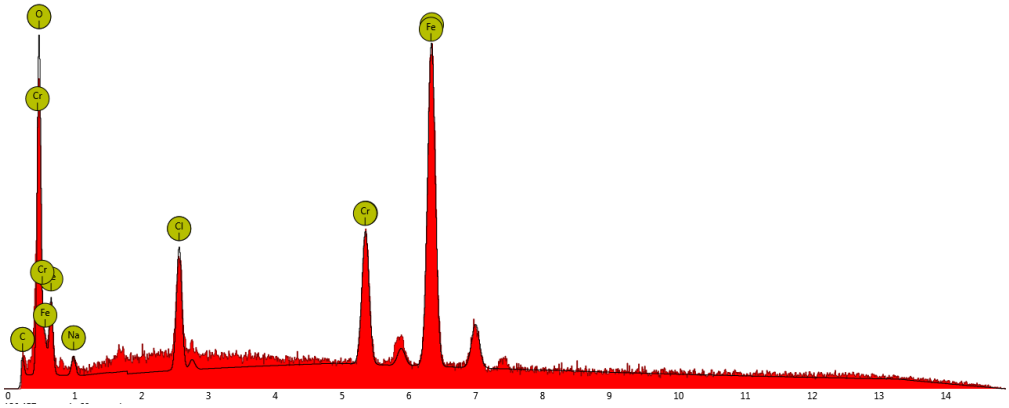

Figure 26 : EDX spectrum result in the corrosion pit for stainless steel 304

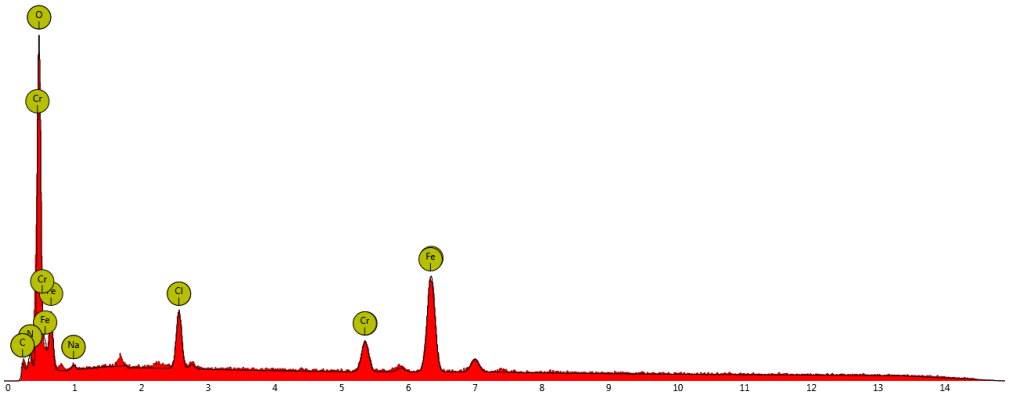

Figure 27 : EDX spectrum result in the corrosion pit for stainless steel 316L

Table 6 : Quantitative EDX result of the corrosion pits for 304 and 316L stainless steel

304	
Element name	Concentration percentage
Iron	55.0
Oxygen	23.9
Chromium	12.5
Chlorine	5.4
Sodium	2.8

316L	
Element name	Concentration percentage
Oxygen	49.7
Iron	35.4
Chromium	6.4
Chlorine	5.2
Sodium	1.4

The composition in the pits were analysed via EDX to determine the content in the pits. EDX was analysed in the red arrow as indicated in Figure 25a and 25b. At 9100x magnification on stainless steel 304, some crack formations were observer in the pits. Both stainless steel 304 and 316L have little corrosion produced outer region of the pits (Figure 25a and Figure 25b). EDX analyse on the pits are display in Figure 26 and Figure 27. The principle consistency of the corrosion on the pits for Stainless steel 304 and 316L pits are oxygen, iron, chromium and chlorine. High content of iron and oxygen in the pits indicate the passive oxide layers were broken down and were reoxidized.

This could be related to the manner that the tests were conducted, since the test was conducted at 100mV as the initial potential which is above the E_{corr} for both stainless steel 304 (E_{corr} -160mV) and 316L (E_{corr} -100mV). Therefore the dominant reactions at this region are the anodic dissolution, which would have broken down the passive oxide film that initiated pits. Once the E_{corr} was achieved, the cathodic reaction of oxidation starts to be the dominant reaction and re-oxidized the pits with oxygen rich compound. A research conducted by A.Pardo on a cyclic polarisation of stainless steel 316 in 3.5% NaCl, indicate that the primary constitution of the corrosion produced of the pits were Cu, Cl and oxygen rich compounds further supports this findings (Pardo, Merino, Carboneras, Coy, & Arrabal, 2007). The drop in E_{corr} in stainless steel 304 could be due to the two different structure of austenite and strain induced martensite present in the microstructure. In studies have shown that the difference in structure creates a galvanic effect between martensite and austenite phase (Hamada, Karjalainen, & Somani, 2006), and further argued that martensite is more negative in the galvanic potential series which increase the susceptibility to pitting corrosion (W. S. Li, Cui, & Luo, 2004).

CHAPTER 5 CONCLUSION

This project paper seeks to understand the natural behaviour of stainless steel in impress current cathodic protection and its effect of cathodic current on it. In order to understand its behaviours, various test were conducted. One of the test is a potentiodynamic test was conducted in a 3.5% NaCl electrolyte in a 1mV/s scanning rate in a potentiostat in order to obtain the polarisation curve.

Various information was extracted from the polarisation curve, such as the corrosion potential and the corrosion current density. The same sample that was used for potentiodynamic testing was than analysed in SEM and EDX.

A few major conclusions have been made with the limited context of the project paper and it is summarised as the following:

- The cathodic polarisation curve of stainless steel 316L and 304 3.5% NaCl were successfully obtained and analysed. The result indicate that the 304 stainless steel (E_{Corr}= -160mV) has a higher corrosion potential compared to 316L (E_{Corr}= -100mV). And this is attributed to the alloying element of 316L stainless steel, which has higher levels of chromium, nickel and molybdenum content. The cathodic reaction of 304stainless steel occurs in a faster rate, with respect to 316L. These reactions are suspected to be dominated pit the pits formation 304 stainless steel. The (i_{corr}) corrosion current density for 304 is 1.6mA/cm^2 and of stainless steel 316L is 2.0mA/cm^2.
- The SEM and EDX result reveals that pitting corrosion were more predominant in stainless steel 304 with respect to 316L. This may be due to a combination of factors such as, stress induced martensite structure in stainless steel 304, alloying

elements, and level of inclusion. The EDX analysis of the pits reveals that the principle constituents are oxygen, iron, chromium, and chlorine. This is an indication of the early stages of pits formation and followed by the cathodic reaction (oxygen reduction).

REFERENCE

Ahmad, Z. (2006). *Principles of Corrosion Engineering and Corrosion Control,*

Alvarez, S. M., Bautista, A., & Velasco, F. (2013). Influence of strain-induced martensite in the anodic dissolution of austenitic stainless steels in acid medium. *Corrosion Science, 69*, 130-138. doi: 10.1016/j.corsci.2012.11.033

ASM. (2000). Introduction to Stainless SteelsAlloy Digest Sourcebook: Stainless Steels (#06940G).

Balasubramaniam, R. (2010). *CALLISTER'S MATERIALS SCIENCE AND ENGINEERING (With CD)*: Wiley India Pvt. Limited.

Barbalat, M., Caron, D., Lanarde, L., Meyer, M., Fontaine, S., Castillon, F., . . . Refait, P. (2013). Estimation of residual corrosion rates of steel under cathodic protection in soils via voltammetry. *Corrosion Science, 73*, 222-229. doi: 10.1016/j.corsci.2013.03.038

Cai, B., Liu, Y., Tian, X., Wang, F., Li, H., & Ji, R. (2010). An experimental study of crevice corrosion behaviour of 316L stainless steel in artificial seawater. *Corrosion Science, 52*(10), 3235-3242. doi: 10.1016/j.corsci.2010.05.040

Chen, X., Li, X. G., Du, C. W., & Cheng, Y. F. (2009). Effect of cathodic protection on corrosion of pipeline steel under disbonded coating. *Corrosion Science, 51*(9), 2242-2245. doi: 10.1016/j.corsci.2009.05.027

Cheng, Y. F., & Niu, L. (2007). Mechanism for hydrogen evolution reaction on pipeline steel in near-neutral pH solution. *Electrochemistry Communications, 9*(4), 558-562. doi: 10.1016/j.elecom.2006.10.035

Crundwell, R. F. (2010). Sacrificial Anodes. In B. C. G. L. L. R. S. Stott (Ed.), *Shreir's Corrosion* (pp. 2763-2780). Oxford: Elsevier.

Dong, C. F., Fu, A. Q., Li, X. G., & Cheng, Y. F. (2008). Localized EIS characterization of corrosion of steel at coating defect under cathodic protection. *Electrochimica Acta, 54*(2), 628-633. doi: 10.1016/j.electacta.2008.07.016

Du, C. W., Li, X. G., Chen, X., Liang, P., & Guo, H. (2008). Crevice corrosion behavior of X70 steel in HCO−3 solution under cathodic polarization. *Acta Metallurgica Sinica (English Letters), 21*(4), 235-244. doi: http://dx.doi.org/10.1016/S1006-7191(08)60044-7

Enos, D. G. (2008). The Potentiodynamic Polarization Scan (Vol. Tehnical Report 33): Center for Electrochemical Science & Engineering, Department of Materials Science & Engineering, University of Virginia, Charlottesville, VA.

Eslami, A., Kania, R., Worthingham, B., Boven, G. V., Eadie, R., & Chen, W. (2011). Effect of CO2 and R-ratio on near-neutral pH stress corrosion cracking initiation under a disbonded coating of pipeline steel. *Corrosion Science, 53*(6), 2318-2327. doi: 10.1016/j.corsci.2011.03.017

Fontana, M. G. (1986). *Corrosion Engineering*: McGraw-Hill.

Freire, L., Carmezim, M. J., Ferreira, M. G. S., & Montemor, M. F. (2011). The electrochemical behaviour of stainless steel AISI 304 in alkaline solutions with different pH in the presence of chlorides. *Electrochimica Acta, 56*(14), 5280-5289. doi: 10.1016/j.electacta.2011.02.094

Genel, K., Demirkol, M., & Ürgen, M. (2002). Effect of cathodic polarisation on corrosion fatigue behaviour of ion nitrided AISI 4140 steel. *International Journal of Fatigue, 24*(5), 537-543. doi: http://dx.doi.org/10.1016/S0142-1123(01)00114-1

Gurrappa, I. (2005). Cathodic protection of cooling water systems and selection of appropriate materials. *Journal of Materials Processing Technology, 166*(2), 256-267. doi: 10.1016/j.jmatprotec.2004.09.074

Hack, H. P. (1999). *Designing Cathodic Protection Systems for Marine Structures and Vehicles*: ASTM.

Hamada, A. S., Karjalainen, L. P., & Somani, M. C. (2006). Electrochemical corrosion behaviour of a novel submicron-grained austenitic stainless steel in an acidic NaCl solution. *Materials Science and Engineering: A, 431*(1-2), 211-217. doi: 10.1016/j.msea.2006.05.138

Hermas, A. A., & Morad, M. S. (2008). A comparative study on the corrosion behaviour of 304 austenitic stainless steel in sulfamic and sulfuric acid solutions. *Corrosion Science, 50*(9), 2710-2717. doi: 10.1016/j.corsci.2008.06.029

Huneau, B., & Mendez, J. (2003). Fatigue behavior of a high strength steel in vacuum, in air and in 3.5% NaCl solution under cathodic protection. *Materials Science and Engineering: A, 345*(1–2), 14-22. doi: http://dx.doi.org/10.1016/S0921-5093(02)00099-0

Huneau, B., & Mendez, J. (2006). Evaluation of environmental effects on fatigue crack growth behaviour of a high strength steel in a saline solution with cathodic protection. *International Journal of Fatigue, 28*(2), 124-131. doi: http://dx.doi.org/10.1016/j.ijfatigue.2005.04.011

Jang, S.-K., Han, M.-S., & Kim, S.-J. (2009). Electrochemical characteristics of stainless steel using impressed current cathodic protection in seawater. *Transactions of Nonferrous Metals Society of China, 19*(4), 930-934. doi: 10.1016/s1003-6326(08)60380-5

Javidi, M., & Bahalaou Horeh, S. (2014). Investigating the mechanism of stress corrosion cracking in near-neutral and high pH environments for API 5L X52 steel. *Corrosion Science, 80*, 213-220. doi: 10.1016/j.corsci.2013.11.031

Jin, G. X., Xie, Y. P., & Tian, A. H. (2012). Corrosion failure analysis of the condensate collector vessel head of evaporation system in ethylene glycol device. *Engineering Failure Analysis, 22*, 113-120. doi: 10.1016/j.engfailanal.2012.01.017

Kim, S.-J., Okido, M., & Moon, K.-M. (2003). An electrochemical study of cathodic protection of steel used for marine structures. *Korean Journal of Chemical Engineering, 20*(3), 560-565. doi: 10.1007/BF02705566

Lei, C., Liu, Y., Zhou, H., Feng, Z., & Du, R. (2013). Photogenerated cathodic protection of stainless steel by liquid-phase-deposited sodium polyacrylate/TiO2 hybrid films. *Corrosion Science, 68*, 214-222. doi: 10.1016/j.corsci.2012.11.019

Li, D. G., Wang, J. D., Chen, D. R., & Liang, P. (2014). Influences of pH value, temperature, chloride ions and sulfide ions on the corrosion behaviors of 316L stainless steel in the simulated cathodic environment of proton exchange membrane fuel cell. *Journal of Power Sources, 272*, 448-456. doi: 10.1016/j.jpowsour.2014.06.121

Li, M. C., & Cheng, Y. F. (2008). Corrosion of the stressed pipe steel in carbonate–bicarbonate solution studied by scanning localized electrochemical impedance spectroscopy. *Electrochimica Acta, 53*(6), 2831-2836. doi: 10.1016/j.electacta.2007.10.077

Li, W. S., Cui, N., & Luo, J. L. (2004). Pitting initiation and propagation of hypoeutectoid iron-based alloy with inclusions of martensite in chloride-containing nitrite solutions. *Electrochimica Acta, 49*(9-10), 1663-1672. doi: 10.1016/s0013-4686(03)01014-4

Lindley, C., & Rudd, W. J. (2001). Influence of the level of cathodic protection on the corrosion fatigue properties of high-strength welded joints. *Marine Structures, 14*(4–5), 397-416. doi: http://dx.doi.org/10.1016/S0951-8339(00)00048-4

Liu, Z. Y., Li, X. G., & Cheng, Y. F. (2011). Electrochemical state conversion model for occurrence of pitting corrosion on a cathodically polarized carbon steel in a near-neutral pH solution. *Electrochimica Acta, 56*(11), 4167-4175. doi: 10.1016/j.electacta.2011.01.100

Liu, Z. Y., Li, X. G., & Cheng, Y. F. (2012a). Mechanistic aspect of near-neutral pH stress corrosion cracking of pipelines under cathodic polarization. *Corrosion Science, 55*, 54-60. doi: 10.1016/j.corsci.2011.10.002

Liu, Z. Y., Li, X. G., & Cheng, Y. F. (2012b). Understand the occurrence of pitting corrosion of pipeline carbon steel under cathodic polarization. *Electrochimica Acta, 60*, 259-263. doi: 10.1016/j.electacta.2011.11.051

Loto, R. T. (2013). Pitting corrosion evaluation of austenitic stainless steel type 304 in acid chloride media. *J. Mater. Environ. Sci. 4 (4) (2013) 448-459, Department of Chemical and Metallurgical Engineering, Tshwane University of Technology, Pretoria, South Africa*.

Matula, M., Hyspecka, L., Svoboda, M., Vodarek, V., Dagbert, C., Galland, J., . . . Tuma, L. (2001). Intergranular corrosion of AISI 316L steel. *Materials Characterization, 46*(2–3), 203-210. doi: http://dx.doi.org/10.1016/S1044-5803(01)00125-5

Metwally, I. A., Al-Mandhari, H. M., Gastli, A., & Nadir, Z. (2007). Factors affecting cathodic-protection interference. *Engineering Analysis with Boundary Elements, 31*(6), 485-493. doi: 10.1016/j.enganabound.2006.11.003

Milad, M., Zreiba, N., Elhalouani, F., & Baradai, C. (2008). The effect of cold work on structure and properties of AISI 304 stainless steel. *Journal of Materials Processing Technology, 203*(1-3), 80-85. doi: 10.1016/j.jmatprotec.2007.09.080

Mustapha, A., Charles, E. A., & Hardie, D. (2012). Evaluation of environment-assisted cracking susceptibility of a grade X100 pipeline steel. *Corrosion Science, 54*, 5-9. doi: 10.1016/j.corsci.2011.08.030

Muthukumaran, V., Selladurai, V., Nandhakumar, S., & Senthilkumar, M. (2010). Experimental investigation on corrosion and hardness of ion implanted AISI 316L stainless steel. *Materials & Design, 31*(6), 2813-2817. doi: 10.1016/j.matdes.2010.01.007

Oni, A. (1996). Effects of cathodic overprotection on some mechanical properties of a dual-phase low-alloy steel in sea water. *Construction and Building Materials, 10*(6), 481-484. doi: http://dx.doi.org/10.1016/0950-0618(95)00086-0

Pardo, A., Merino, M. C., Carboneras, M., Coy, A. E., & Arrabal, R. (2007). Pitting corrosion behaviour of austenitic stainless steels with Cu and Sn additions. *Corrosion Science, 49*(2), 510-525. doi: 10.1016/j.corsci.2006.06.004

Pardo, A., Merino, M. C., Coy, A. E., Viejo, F., Arrabal, R., & Matykina, E. (2008a). Effect of Mo and Mn additions on the corrosion behaviour of AISI 304 and 316 stainless steels in H2SO4. *Corrosion Science, 50*(3), 780-794. doi: 10.1016/j.corsci.2007.11.004

Pardo, A., Merino, M. C., Coy, A. E., Viejo, F., Arrabal, R., & Matykina, E. (2008b). Pitting corrosion behaviour of austenitic stainless steels – combining effects of Mn and Mo additions. *Corrosion Science, 50*(6), 1796-1806. doi: 10.1016/j.corsci.2008.04.005

Park, H., Kim, K. Y., & Choi, W. (2001). A novel photoelectrochemical method of metal corrosion prevention using a TiO2 solar panel. *Chemical Communications*(3), 281-282.

Park, H., Kim, K. Y., & Choi, W. (2002). Photoelectrochemical approach for metal corrosion prevention using a semiconductor photoanode. *Journal of Physical Chemistry B, 106*(18), 4775-4781. doi: 10.1021/jp025519r

Perdomo, J. J., & Song, I. (2000). Chemical and electrochemical conditions on steel under disbonded coatings: the effect of applied potential, solution resistivity, crevice thickness and holiday size. *Corrosion Science, 42*(8), 1389-1415. doi: http://dx.doi.org/10.1016/S0010-938X(99)00136-5

Roberge, P. (1999). *Handbook of Corrosion Engineering*: Mcgraw-hill.

Roberge, P. R. (2000). Handbook of Corrosion Engineering. *11. Cathodic protection*.

Roffey, P., & Davies, E. H. (2014). The generation of corrosion under insulation and stress corrosion cracking due to sulphide stress cracking in an austenitic stainless steel hydrocarbon gas pipeline. *Engineering Failure Analysis, 44*, 148-157. doi: 10.1016/j.engfailanal.2014.05.004

Shipilov, S. A., & Le May, I. (2006). Structural integrity of aging buried pipelines having cathodic protection. *Engineering Failure Analysis, 13*(7), 1159-1176. doi: 10.1016/j.engfailanal.2005.07.008

Smith, W. F. (1993). *Structure and Properties of Engineering Alloys*: McGraw-Hill.

Solheim, K. G., & Solberg, J. K. (2013). Hydrogen induced stress cracking in supermartensitic stainless steels – Stress threshold for coarse grained HAZ. *Engineering Failure Analysis, 32*, 348-359. doi: 10.1016/j.engfailanal.2013.04.003

Song, F. M., & Sridhar, N. (2008). Modeling pipeline crevice corrosion under a disbonded coating with or without cathodic protection under transient and steady state conditions. *Corrosion Science, 50*(1), 70-83. doi: 10.1016/j.corsci.2007.05.024

Wang, W., Wang, Q., Wang, C., & Yi, J. (2014). Experimental studies of crevice corrosion for buried pipeline with disbonded coatings under cathodic protection. *Journal of Loss Prevention in the Process Industries, 29*, 163-169. doi: 10.1016/j.jlp.2014.02.007

William Smith, W. F. (1993). *Structure and Properties of Engineering Alloys Second Edition* McGraw-Hill.

Xin, S. S., & Li, M. C. (2014). Electrochemical corrosion characteristics of type 316L stainless steel in hot concentrated seawater. *Corrosion Science, 81*, 96-101. doi: 10.1016/j.corsci.2013.12.004

Xu, C., Zhang, Y., Cheng, G., & Zhu, W. (2008). Pitting corrosion behavior of 316L stainless steel in the media of sulphate-reducing and iron-oxidizing bacteria. *Materials Characterization, 59*(3), 245-255. doi: 10.1016/j.matchar.2007.01.001

Xu, L. Y., Su, X., & Cheng, Y. F. (2013). Effect of alternating current on cathodic protection on pipelines. *Corrosion Science, 66*(0), 263-268. doi: http://dx.doi.org/10.1016/j.corsci.2012.09.028

Yuan, J., & Tsujikawa, S. (1995). Characterization of sol-gel-derived TiO2 coatings and their photoeffects on copper substrates. *Journal of the Electrochemical Society, 142*(10), 3444-3450.

Zakroczymski, T., & Owczarek, E. (2002). Electrochemical investigation of hydrogen absorption in a duplex stainless steel. *Acta Materialia, 50*(10), 2701-2713. doi: http://dx.doi.org/10.1016/S1359-6454(02)00105-2

Zhiyong, L., Zhongyu, C., Xiaogang, L., Cuiwei, D., & Yunying, X. (2014). Mechanistic aspect of stress corrosion cracking of X80 pipeline steel under non-stable cathodic polarization. *Electrochemistry Communications, 48*(0), 127-129. doi: http://dx.doi.org/10.1016/j.elecom.2014.08.016

Ziaei, S. M. R., Mostowfi, J., Golestani pour, M., & Ziaei, S. A. R. (2013). Failure analysis: Chloride stress corrosion cracking of AISI 316 stainless steel downhole pressure memory gauge cover. *Engineering Failure Analysis, 33*, 465-472. doi: 10.1016/j.engfailanal.2013.06.022

Zucchi, F., Grassi, V., Monticelli, C., & Trabanelli, G. (2006). Hydrogen embrittlement of duplex stainless steel under cathodic protection in acidic artificial sea water in the presence of sulphide ions. *Corrosion Science, 48*(2), 522-530. doi: 10.1016/j.corsci.2005.01.004